

Frustrated Quantum Magnets in 2d: from Néel phases to Spin Liquids

Claire Lhuillier

Université P. et M. Curie (Paris VI) and Institut Universitaire de France

Laboratoire de Physique Théorique de la matière Condensée

UMR 7600 of CNRS,

case 121, 4 Place Jussieu,

75252 Paris Cedex

email: claire.lhuillier@upmc.fr

June 2, 2006

Abstract

A description of different phases of two dimensional magnetic insulators is given.

The first chapter is devoted to the understanding in an $SU(2)$ invariant picture of the most standard antiferromagnetic scheme originating from Néel: this give light both on the spectra of molecular magnets and on the symmetry breaking mechanism in the semi-classical Néel phases. The description of the ground-state wave-functions in term of Valence-Bond is emphasized. Different scenarii leading to restoration of $SU(2)$ symmetry are examined: in particular the possibility of a two step scenario with an intermediate nematic phase is illustrated. The excitations of the different symmetry breaking phases are described.

Different gapful quantum phases exist in two dimensions: the Valence Bond Crystal phases (VBC) which have long range order in local $S=0$ objects (either dimers in the usual Valence Bond acception or quadrumers..), but also Resonating Valence Bond Spin Liquids (RVBSL), which have no long range order in any local order parameter and an absence of susceptibility to any local probe. VBC have gapful integer spin excitations, RVBSL on the contrary have deconfined spin-1/2 excitations. Examples of these two kinds of quantum phases are given in chapters 2 and 3.

Contents

1	<i>SU</i>(2) symmetry breaking phases:	
	Ground-state wave-functions and excitations in an <i>SU</i>(2) invariant approach	5
1.1	A simple exactly solvable model	5
1.1.1	Introduction of a toy model: the rigid Macro-antiferromagnet	5
1.1.2	Ground-state(s) and excitations of the rigid Macro-Antiferromagnet	7
1.2	From the classical to the semi-classical Néel antiferromagnet .	11
1.2.1	Adiabatic continuation scenario from the classical rigid antiferromagnet to the semi-classical Néel state of the Heisenberg model	11
1.2.2	Finite size scalings	12
1.2.3	Self-consistency magnon description in the <i>SU</i> (2) invariant picture.	14
1.3	When the adiabatic continuation scenario fails	19
1.3.1	Order from disorder selection	19
1.3.2	A partial restoration of the <i>SU</i> (2) symmetry by quantum fluctuations: the p-nematic magnet	20
1.3.3	Full destruction of the semi-classical phases by quantum fluctuations: VBC and RVB phases	28
1.3.4	Some omissions, and relevant refs.	29
1.4	Complement-1 A simple conceptual approach of the translational symmetry breaking in a solid	30
1.4.1	An essential classical hypothesis	30
1.4.2	Quantization of the classical approach, finite size spectra, thermodynamic limit and translational symmetry breaking	31
1.4.3	Thermodynamic limit, stability of the solid and self-consistency of the approach	33
1.5	Complement-2: <i>SU</i> (2) symmetry breaking in the Néel antiferromagnet	33

2	Valence Bond Crystals	35
2.1	1-dimensional VBC	35
2.2	A quick glance on two-dimensional VBC	36
2.2.1	The $J_1 - J_2$ model on the square lattice	36
2.2.2	More consensual examples: from strong coupling solutions to explicit VBC	38
2.2.3	Spontaneous VBC	38
2.3	The Heisenberg model on the checker-board lattice: an example of a Valence Bond Crystal	39
2.3.1	Classical ground-states	39
2.3.2	The Quantum HCKB model: Spin Gap	39
2.3.3	Degeneracy of the ground-state and space symmetry breaking in the thermodynamic limit	40
2.3.4	Excitations: raw data and qualitative description of the first excitations	42
2.4	Valence Bond Solids	44
2.5	Summary of the properties of VBC phases	45
2.6	A simple model of VBC with a critical point: the hard core quantum dimer model of Rokhsar and Kivelson on the square lattice	46
2.6.1	Hilbert space and Hamiltonian of quantum dimer models	46
2.6.2	Topological structure of the Hilbert space of the QDM model on the square lattice	47
2.6.3	Phase Diagram of the RK model	48
3	Resonating Valence Bond Spin Liquids	50
3.1	Introduction: short range versus long range Resonating Valence Bond wave-functions	51
3.2	The Quantum Dimer Model on the triangular lattice	52
3.3	Solvable QDM on the kagome lattice	54
3.3.1	Hamiltonian	54
3.3.2	RK ground-state	55
3.3.3	Ising pseudo-spin variables	56
3.3.4	Dimer-dimer correlations	57
3.3.5	Visons excitations	57
3.3.6	Spinons deconfinement	59
3.3.7	\mathbb{Z}_2 gauge theory	60
3.4	Summary of properties of RVB Spin liquids	61

Chapter 1

$SU(2)$ symmetry breaking phases: Ground-state wave-functions and excitations in an $SU(2)$ invariant approach

In this chapter we want to uncover in a very simple quantum mechanical $SU(2)$ invariant point of view, the nature of the semi-classical symmetry breaking phases and the mechanism of the $SU(2)$ symmetry breaking. This will shed light on the spectrum of nanomagnets, on the structure of the ground-state wave function of the Néel states in term of valence-bonds and on the possible scenarii leading from Néel states to $SU(2)$ non breaking phases.

1.1 A simple exactly solvable model

1.1.1 Introduction of a toy model: the rigid Macro-antiferromagnet

Let us consider the Heisenberg hamiltonian:

$$\mathcal{H} = 2J \sum_{\langle i,j \rangle} \mathbf{s}_i \cdot \mathbf{s}_j \quad (1.1)$$

where $\mathbf{s}_i, \mathbf{s}_j$ are spins $1/2$, the sum $\langle i, j \rangle$ runs on pairs of next neighbor sites and J measures the strength of the effective coupling.

On a lattice of N sites with periodic boundary conditions, this hamiltonian reads in reciprocal space:

$$\mathcal{H} = 2J \sum_{k \in Bz} \gamma_k \tilde{\mathbf{S}}_k \cdot \tilde{\mathbf{S}}_{-k}. \quad (1.2)$$

In this expression:

$$\tilde{\mathbf{S}}_k = \frac{1}{\sqrt{N}} \sum_i \mathbf{s}_i \exp(-i\mathbf{k}\cdot\mathbf{r}_i) \quad (1.3)$$

where \mathbf{r}_i is the coordinate of spin i , N the number of lattice sites and \mathbf{k} runs on the reciprocal points of the lattice in the first Brillouin zone (Bz). γ_k is the structure factor of the lattice:

$$\gamma_k = \frac{1}{2} \sum_{i=1,2} \cos(\mathbf{k}\cdot\mathbf{e}_i) \quad (1.4)$$

with \mathbf{e}_j , ($j = 1, 2$), the unit vectors generating the 2-dimensional lattice.

For simplicity we will specialize to the square lattice case.¹ On this lattice the Néel state is invariant by 2-step translations associated to wave-vectors $\mathbf{0} = (0, 0)$ and $\mathbf{k}_0 = (\pi, \pi)$. Let us select these special components in the Heisenberg Hamiltonian and rewrite it as:

$$\mathcal{H} = \mathcal{H}_0 + \mathcal{V} \quad (1.6)$$

with

$$\mathcal{H}_0 = 2J(\tilde{\mathbf{S}}_0^2 - \tilde{\mathbf{S}}_{\mathbf{k}_0} \cdot \tilde{\mathbf{S}}_{-\mathbf{k}_0}) \quad (1.7)$$

$$\mathcal{V} = 2J \sum_{\mathbf{k} \in Bz^*} \gamma_k \tilde{\mathbf{S}}_{\mathbf{k}} \cdot \tilde{\mathbf{S}}_{-\mathbf{k}} \quad (1.8)$$

where Bz^* is to be understood as the first Brillouin zone minus the $\mathbf{k} = \mathbf{0}$ and \mathbf{k}_0 points.

It is straightforward to show that:

$$\begin{aligned} \mathcal{H}_0 &= \frac{4J}{N} (\mathbf{S}_{tot}^2 - \mathbf{S}_A^2 - \mathbf{S}_B^2) \\ &= \frac{8J}{N} \mathbf{S}_A \cdot \mathbf{S}_B \end{aligned} \quad (1.9)$$

where \mathbf{S}_{tot} is the total spin of the sample and $\mathbf{S}_{A,B}$ the total spins of the A , and B sublattices. We will call this model the rigid Macro-Antiferromagnet.²

¹The same kind of toy model can be introduced in the 3-sublattice Néel state on a triangular lattice: in that last case it involves the Fourier components of the spins at the three soft points (which are the center and the two non equivalent corners of the Brillouin zone) and reads:

$$\mathcal{H}_0^{tri} = \frac{9J}{2N} (\mathbf{S}_{tot}^2 - \mathbf{S}_A^2 - \mathbf{S}_B^2 - \mathbf{S}_C^2) \quad (1.5)$$

where $\mathbf{S}_{A,B,C}$ are the total spins of the A , B , C sublattices. Such a model allows the same developments as those done below except indeed the comments on the Lieb-Mattis ordering theorem [1].

²You can recognize in \mathcal{H}_0 the model used by Lieb and Mattis in the demonstration of the ordering theorem [2]. For bipartite lattices this theorem originally due to Hulthén (1938)[3], Marshall (1955)[4] and strengthened by Lieb and Mattis (1962)[2] states that

This model describes a problem with constant infinite range interactions between spins on different sublattices and no interactions between spins on the same sublattice. It has a correct thermodynamic limit, and can be solved exactly.

1.1.2 Ground-state(s) and excitations of the rigid Macro-Antiferromagnet

Hamiltonian \mathcal{H}_0 (Eq. 1.9) is an $SU(2)$ invariant Hamiltonian which commutes with \mathbf{S}_{tot}^2 and \mathbf{S}_{tot}^z . It also commutes with $\mathbf{S}_{A,B}^2$, which in this model are conservative quantities (good quantum numbers). From now on, for notation simplicity we will drop the underscored *tot* for the total spin.

Eigen-states of \mathcal{H}_0 are build from the addition of the two big spins $\mathbf{S}_{A,B}$ and have eigen-values:

$$E(S, S_A, S_B) = \frac{4J}{N} [S(S+1) - S_A(S_A+1) - S_B(S_B+1)] \quad (1.11)$$

The quantum numbers labelling these eigenstates on a sample with an (even) number of sites N are:

the values of the sublattice magnetisations: $S_A, S_B, \in [0, 1, \dots, N/4]$,

the value of the total spin: $S \in [|S_A - S_B|, \dots, S_A + S_B]$,

and the value of its z component $M_S : \in [-S, -S+1, \dots, S-1, S]$.

From now on I will note these eigenstates: $|S_A, S_B, S, M_S \rangle$.

The absolute ground-state

From Eq. 1.11 it appears that the absolute ground-state is obtained for the maximum polarisation of the two sublattices $S_A = S_B = N/4$ and a total spin $S = 0$.

- This ground-state

$$|0, 0 \rangle = |S_A = N/4, S_B = N/4, S = 0, M_S = 0 \rangle \quad (1.12)$$

is the $S = 0$, $SU(2)$ invariant component of the usual Ising antiferromagnet wave-function:

$$|Ising A.F. \rangle = \prod_{i \in A, j \in B} |i, + \rangle |j, - \rangle. \quad (1.13)$$

the absolute ground-state of the antiferromagnetic Heisenberg (1.1) (and of more general antiferromagnetic models respecting the bipartition of the lattice) is unique and has total spin zero. Moreover the ground-state energies in each S sector are ordered accordingly to S_{tot} :

$$\forall S'_{tot} > S_{tot} \quad E_0(S'_{tot}) > E_0(S_{tot}). \quad (1.10)$$

Usual the basic relations for angular momentum addition, the Ising antiferromagnet wave-function can be written:

$$\begin{aligned}
|Ising A.F. \rangle &= \\
&\sum_{S, M_S} \langle S_A, S_B, S, M_S | S_A, M_A, S_B, M_B \rangle |S_A, S_B, S, M_S \rangle \\
&= \sum_{S, M_S} \frac{(-1)^{M_S}}{\sqrt{2S+1}} \begin{pmatrix} S_A & S_B & S \\ S_A & -S_B & M_S \end{pmatrix} |S_A, S_B, S, M_S \rangle \quad (1.14)
\end{aligned}$$

where $S_A = S_B = N/4$, $M_A = N/4$, $M_B = -N/4$.

$\langle S_A, S_B, S, M_S | S_A, M_A, S_B, M_B \rangle$ are known in elementary quantum mechanics as the Clebsch-Gordan coefficients. ³

- The absolute ground-state wave-function (Eq.1.12) can also be written as a linear superposition of products of **valence-bonds** (singlet pairs of the individual spin-1/2). Let us do it by using the projectors on the irreducible representations (irreps) of the permutation group in terms of Young tableaux.

The $S = 0$ wave functions belong to the irrep associated to the Young tableau with $N/2$ columns and 2 lines. The wave-function given by (Eq.1.12) is totally symmetric in the exchange of spins in any of the two sublattices (these sublattices are ferromagnetically aligned) and, it is a $S=0$ wave function, antisymmetric in the permutation of any pairs of spins belonging to different sublattices. As this wave-function is unique (there is only one way to couple two given spins S_A, S_B in a given total spin S), it may also be described by using first the antisymmetrizers on spins of different sublattices, which creates a product of $N/2$ valence-bonds, followed by the symmetrisation on all spins of each A and B sublattices.

This shows that Eq.1.12 can also be written as an equal weight superposition of all the products of valence-bonds that could be drawn between the A and B sublattices. This wave-function belongs to the variational sub-space studied by Liang, Douçot and Anderson in 1988 [5]: with the special property that the weights of all bonds, whatever their length are equal.

Ground-states of all S sectors

From Eq. 1.11 it appears that the ground-state $E_0(S)$ of the sector with total spin S is the state $|S_A, S_B, S, M_S \rangle$ with maximum sublattice magnetizations $N/4$. These eigen-states are also the $SU(2)$ invariant components of the Ising Antiferromagnet (Eq. 1.14).

³These coefficients are the coefficients of the unitary transformation which transforms the uncoupled sublattice spins $S_{A,B}$ to the $SU(2)$ invariant coupled combinations. They are related to the Wigner “3j” symbols (second line) that can be calculated by elementary algebra, and are tabulated in books and in computer libraries.

The energies of these low energy states obey the following relation:

$$E_0(S) = -\frac{J}{2}(N+4) + \frac{4J}{N}[S(S+1)] \quad (1.15)$$

They collapse to the absolute ground-state as $\mathcal{O}(\frac{S(S+1)}{N})$. On a finite size lattice the classical Néel state (1.14) is a non stationary state of \mathcal{H}_0 (1.9). But, its precession rate decreases as $\mathcal{O}(\frac{1}{N})$ with the system size and becomes infinitely slow in the thermodynamic limit. This property is the basis of the $SU(2)$ symmetry breaking in the Néel states.

In the following I will call this family of levels the "Anderson tower of states" in honor to P.W. Anderson 1952 famous paper on spin-waves in antiferromagnets [6] where their necessary existence is discussed for the first time (?) in a tiny footnote at the end of the paper. ⁴

This approach and its extensions to more complex Néel order parameters show that **the multiplicity of the Néel ground-state subspace in the thermodynamic limit is $\mathcal{O}(N^\alpha)$, where α is the number of sublattices of the classical Néel state**[1, 8]. This gives a non extensive entropy of the ground-state at $T = 0$ in agreement with Nernst theorem.

A last important remark: the homogeneous spin susceptibility is always dominated by the largest spin states of the Anderson tower: that is states with total spin $\mathcal{O}(\sqrt{N})$. Most of the macroscopic measurement will equally be dominated by these levels. In bulk materials a state with total spin \sqrt{N} has a very large spin, it is essentially a classical object but its magnetization by site: $m = S_{tot}/\frac{N}{2} \propto \frac{1}{\sqrt{N}}$, that is essentially zero in the thermodynamic limit.

Excitations

In this model an excited state is obtained by flipping a single spin of a sublattice ($\Delta S_{A,B} = -1$ and $\Delta S^z = +1$, arrow in Fig.1.1). From equation (1.11) one sees that these excitations are highly degenerate, localized and have an energy:

$$E^{ex} = 2J \left[1 + \frac{4(S+1)}{N} \right]. \quad (1.16)$$

For any system size these excitations are gapful and $\mathcal{O}(J)$.

In spite of the $SU(2)$ invariant feature of the model, its low energy excitations are similar to those of the Ising model. *And in spite of the possible continuous symmetry breaking, there is no Goldstone modes. It is a consequence of the infinite range of the interactions.*

⁴In our first paper[7] we have called these levels QDJS (for quasi degenerate joint states). I was told that nuclear physicists have also their own words to describe the same phenomenon.

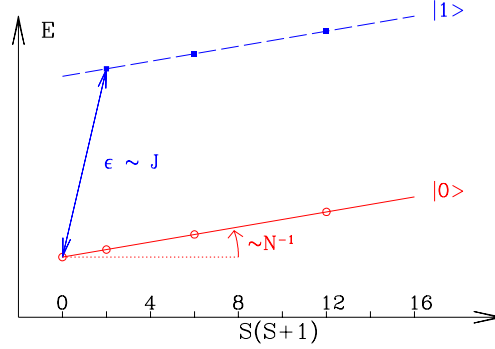


Figure 1.1: Typical spectrum of a finite size collinear Ising magnet. The tower of eigen-levels joined by the continuous line and noted $|0\rangle$ is the Anderson tower of states needed to form a symmetry breaking Ising ordered ground-state (Eq. 1.19): such a state is non stationary on a finite size sample. The second set $|1\rangle$ (dashed line) is associated with the lowest excitations, which are highly degenerate and non dispersive.

Conclusion

\mathcal{H}_0 describes a classical rigid antiferromagnet in an $SU(2)$ invariant framework: its spectrum has the very simple structure schematized in Fig. 1.1. In the thermodynamic limit this magnet can be described either in an $SU(2)$ invariant language with the help of the $|S_A, S_B, S, M_S\rangle$ states or with the coherent classical Néel states pointing along the \mathbf{u} direction:

$$|\text{ClassicalNéelA.F.}\mathbf{u}\rangle = e^{iS_{\text{tot}}^z \phi} e^{iS_{\text{tot}}^y \theta} |\text{IsingA.F.}\rangle \quad (1.17)$$

where θ and ϕ are the Euler angles of \mathbf{u} .⁵ In the thermodynamic limit, the symmetry breaking point of view is as valid as the $SU(2)$ invariant approach.

⁵These states form an (overcomplete) basis of the thermodynamic ground-state multiplicity. The two basis are connected by exact transformation laws, Eq.(1.14) and its inverse:

$$|N/4, N/4, S, M_S\rangle = (2S+1) \int d\tau D_S^\dagger(\phi, \theta) |\text{Cl. Néel w.f.}; \mathbf{u}\rangle, \quad (1.18)$$

where the differential integration volume reads $d\tau = \frac{1}{4\pi} d\phi d(\cos\theta)$, where $\phi \in [0, 2\pi]$, $\theta \in [0, \pi]$ and D_S is the rotation matrix in the S subspace.

1.2 From the classical to the semi-classical Néel antiferromagnet

Modification of this picture in an Heisenberg magnet with next neighbor exchange comes from the effect of the perturbation \mathcal{V} described in Eq. 1.8. \mathcal{V} does not commute with \mathbf{S}_A^2 and \mathbf{S}_B^2 : at first order in perturbation each component of \mathcal{V} couples the ground-states of \mathcal{H}_0 of each S sector to states where the sublattice magnetizations are decreased by one unit in some modulated way: the first effect of the perturbation is thus to reduce the sublattice magnetizations.

1.2.1 Adiabatic continuation scenario from the classical rigid antiferro-magnet to the semi-classical Néel state of the Heisenberg model

The semi-classical Néel state, if it exists, emerges from the dressing of the Anderson tower of states of the toy model by the quantum fluctuations produced by \mathcal{V} . The adiabatic continuation from one ground-state multiplicity to the other implies the qualitative conservation of the structure and of the spectrum of the Anderson tower of states of the macroscopic ground-state: i.e.

- Exact conservation of the number and spatial symmetries of the low lying states in each S sector,
- Scaling of these levels as $\mathcal{O}(\frac{JS(S+1)}{N})$ with respect to the ground-state,
- Robustness in each of these states of a macroscopic sublattice magnetization: $\sqrt{\langle S_A^2 \rangle} \propto \mathcal{O}(N)$.⁶

If there is an adiabatic continuation between the two models the quantum Néel wave-function will read:

$$|Qu. Néel w.f. \rangle = \sum_{S, M_S} \frac{(-1)^{M_S}}{\sqrt{2S+1}} \begin{pmatrix} S_A & S_B & S \\ S_A & -S_B & M_S \end{pmatrix} |\widetilde{S}, \widetilde{M}_S \rangle_0 \quad (1.19)$$

where the kets $|\widetilde{S}, \widetilde{M}_S \rangle_0$ are now the exact low lying states of the Anderson tower of \mathcal{H} (Eq. 1.1).

To check if the adiabatic continuation fails or not, there are 2 possible routes, exact diagonalisations or perturbation theory, which in fact reinforce each other. A correct interpretation of the exact diagonalization data implies a relevant study of the finite size effects. We will therefore develop the

⁶As an example, all these criteria have been thoroughly checked in the Néel ordered phase of the Heisenberg model on the triangular lattice[7, 1]

qualitative feature of the finite size scaling laws using well known results of spin wave theory.⁷

1.2.2 Finite size scalings

Let us recall the main results of the spin-wave calculation. (For the derivation of the spin-wave approach in antiferromagnets, see text-books [15, 16, 17].)

Departing from the Ising configuration (Eq.1.13), the transverse terms of the Heisenberg Hamiltonian create $\Delta S^z = 1$ spin flips, which are mobile excitations.

- In an harmonic approximation these excitations are simply described as bosons, with frequencies:

$$\omega_{\mathbf{q}} = 2J\sqrt{1 - \gamma_{\mathbf{q}}^2} \quad (1.20)$$

where $\gamma_{\mathbf{q}}$ is the structure factor of the lattice defined in Eq.(1.4). The spin flips excitations are then dispersive, their frequency goes to zero when going to the two soft points $\mathbf{k} = \mathbf{0}, \mathbf{k}_0$. Around these points the dispersion law is linear in \mathbf{k} (resp. $(\mathbf{k} - \mathbf{k}_0)$).

- The zero point energy of these excitations (which are oscillator- like) renormalizes the Ising classical energy of the ground-state. To first order, this spin wave calculation gives the ground-state energy of the Heisenberg Hamiltonian on the square lattice as:

$$E^{sw} = -\frac{N}{2}z\frac{J}{4} - NJ + \sum_{\mathbf{q} \in BZ^*} \frac{\omega_{\mathbf{q}}}{2} \quad (1.21)$$

where z is the coordination number of the lattice.

- These “quantum fluctuations” also renormalize the sublattice magnetization. The order parameter m reads:

$$m^{sw} = \frac{2}{NS} \langle sw - gs | S_A^z | sw - gs \rangle \simeq 1 - \frac{1}{N} \sum_{\mathbf{q} \in BZ^*} \left[\frac{1}{\omega_{\mathbf{q}}} - 1 \right]. \quad (1.22)$$

The renormalization of the order parameter is dominated by the fluctuations in the low energy modes. The linear asymptotic behavior of

⁷More sophisticated approaches [9, 10, 11, 12, 13, 14] would lead to the same qualitative results with more efforts. Having explicitated the equivalence between the $SU(2)$ invariant Anderson tower of states and the symmetry breaking states, we can indeed extract the finite size scaling laws from the technically more convenient point of view. Moreover our approach shows that renormalization by quantum fluctuations primarily acts on the macroscopic sublattices spins: by the way the spin-wave approach takes in this point of view a deeper justification than in other usual introductions.

Lattices	Coordination number	$2 \langle \mathbf{S}_i \cdot \mathbf{S}_j \rangle$ per bond	M/M_{cl}	
dimer	1	-1.5		
1 square	2	-1		
1 D Chain	2	-0.886	0	
honeycomb [18]	3	-0.726	0.44	bipartite lattices
sq-hex-dod. [19]	3	-0.721	0.63	
square [20]	4	-0.669	0.60	
classical value		-0.5	1	
one triangle	2	-0.5		
kagome [21]	4	-0.437	0	frustrating lattices
triangular [1]	6	-0.363	.50	
classical value		-0.25	1	
1 tetrahedron	3	-0.5		
checker-board [22]	6	-0.343	0	frustr. latt.

Table 1.1: Quantum energy per bond and sublattice magnetization in the ground-state of the spin-1/2 Heisenberg Hamiltonian on various simple cells and lattices. The sq-hex-dod. is a bipartite lattice formed with squares, hexagons and dodecagons.

$\omega_{\mathbf{q}}$ around the soft points, implies that the spin-waves correction to the order parameter diverges in 1D. It gives finite corrections at $T = 0$ on most 2-dimensional lattices (square, triangular, hexagonal).⁸ This scenario is fully supported by exact diagonalizations as displayed in Table 1.1.

- **Finite size effects:** On a finite $L \times L$ lattice, the allowed wave vectors are quantized and $\propto \frac{2\pi}{L}$. This infra-red cut-off of the long wave-length fluctuations is progressively relaxed as the size of the sample goes to ∞ . As $\omega_{\mathbf{q}}$ is linear in \mathbf{q} around the soft points, the ground-state energy E^{sw} (Eq. 1.21) and the order parameter m^{sw} (Eq. 1.22) differ from the $L \rightarrow \infty$ limits by factors of order $\mathcal{O}(\frac{1}{L})$.

Let us also emphasize that on a finite lattice the energy needed to create the softest excitation is of order $\frac{J}{L} \propto \frac{J}{N^{1/d}}$.

⁸The exceptions: the checker-board and the kagome lattice will be studied in forthcoming sections.

1.2.3 Self-consistency magnon description in the $SU(2)$ invariant picture.

If the structure of the tower of states is essentially preserved by the quantum fluctuations due to \mathcal{V} , the semi-classical picture of coherent states is preserved, the spin-wave approach is a reasonable one and the essential results of this approach should appear in the full spectra of Eq.(1.1). Beyond the criteria already described in subsection 1.2.1 to support the $SU(2)$ symmetry breaking in the macroscopic ground-state, the following structure and size effects characterize the magnons in the $SU(2)$ invariant picture:

- The softest magnon with wave-vector $\frac{2\pi}{L}$ is described by a second tower of states issued from the tower of excited states of the Ising model with one spin-flip (Eq. 1.16) (line $|1 \rangle$ of Fig. 1.2), and the levels in this second tower of states equally collapse as $1/N$ in the thermodynamic limit.
- But contrary to the Ising model, these states are now dispersive and the lowest excitation is now distant from the ground-state tower of states by an energy of the order of $\frac{J}{L}$: it is the Goldstone mode of the broken $SU(2)$ symmetry.

Some of these properties are summarized in the supposed-to-be spectrum of a Néel antiferromagnet described in Fig. 1.2 . This is to be compared to exact spectra of the Heisenberg Hamiltonian on a square lattice (Fig. 1.3)[23] or on an hexagonal lattice (Figs. 1.4, 1.5, 1.6) [18].

A new light on the Mermin-Wagner theorem

The levels of the Anderson towers (of the macroscopic ground-state and of the magnons), collapse as $\mathcal{O}(1/N)$. The ground-state multiplicity is separated from the softest magnon multiplicity by an energy $\mathcal{O}(1/L)$. If $d \geq 2$, the $SU(2)$ symmetry breaking could be achieved without ambiguity and the semi-classical picture is justified. On the other hand if $d = 1$, there is no way to disentangle the different classes of eigen-states and the picture breaks down. This approach gives thus a new light on the Mermin-Wagner theorem which denies the existence of Néel long range order in 1 dimensional magnets.

This global understanding of the spectra of finite size samples of antiferromagnets is a very useful tool to analyze exact spectra of spin models that can be obtained with present computer facilities⁹. It may probably help to understand the time behavior of nano-scale $SU(2)$ invariant antiferromagnets [25, 26, 27, 28].

⁹Historically the first authors to have looked for the Anderson tower of states were probably A. Sütö and P. Fazekas in 1977 [24], and with the modern computational facilities M. Gross, E. Sanchez-Velasco and E. Siggia [9, 10].

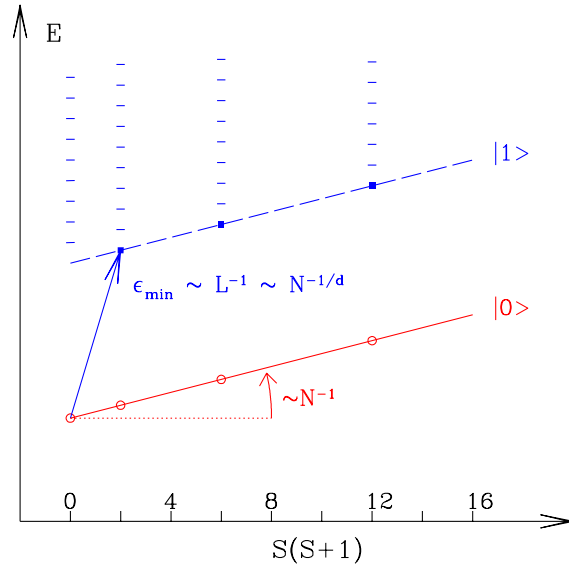


Figure 1.2: Typical spectrum of a finite size collinear antiferromagnet with Néel order. The tower of eigen-levels joined by the continuous line and noted $|0\rangle$ is the Anderson tower of states needed to form a symmetry breaking Néel ordered ground-state (Eq. 1.19): such a state is non stationary on a finite size sample. The second set $|1\rangle$ (dashed line) is associated with the softest magnon of the sample.

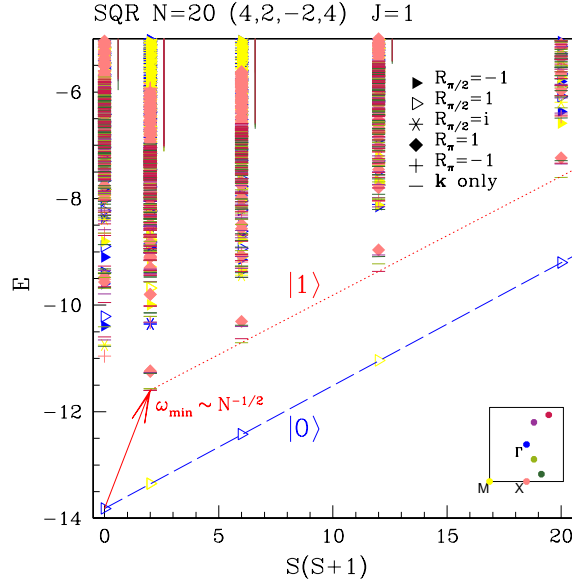


Figure 1.3: Results of exact diagonalizations of the Antiferromagnetic Heisenberg model on the square lattice: eigen-energies vs eigen-values of \mathbf{S}^2 . The dashed-line is a guide to the eyes through the levels of the Anderson towers of state of the macroscopic ground-state. The dotted line joins the states associated to the first magnon. In the ground-state tower there is one eigenlevel for each S (as expected for a collinear antiferromagnet). Depending on the parity of the total spin it is a $\mathbf{k} = \mathbf{0}$ state or $\mathbf{k} = (\pi, \pi)$ state, invariant in C_4 rotations.

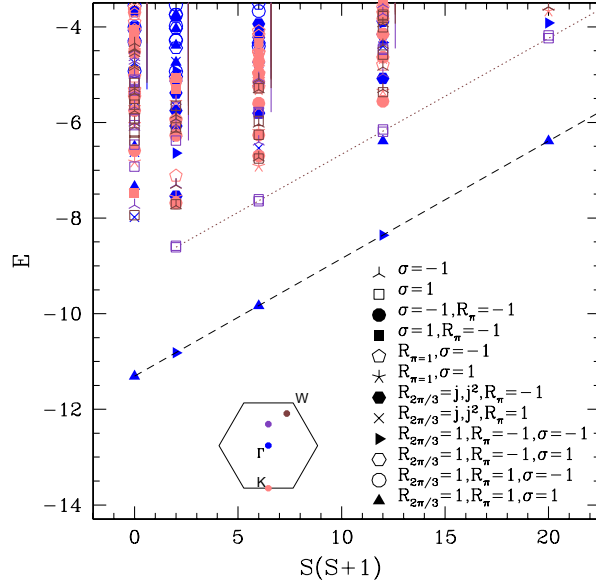


Figure 1.4: Antiferromagnetic Heisenberg model on the honeycomb lattice: eigen-energies vs eigen-values of S^2 . The dashed-line is a guide to the eyes for the QDJS. The dotted line joins the states associated to the first magnon. There is one QDJS for each S (as expected for a collinear antiferromagnet): they are $\mathbf{k} = \mathbf{0}$ states, invariant under a $2\pi/3$ rotation around an hexagon center, even (odd) under inversion, odd (even) under a reflection with respect to an axis going through nearest neighbor hexagon centers for S even (odd) (taken from ref. [18]).

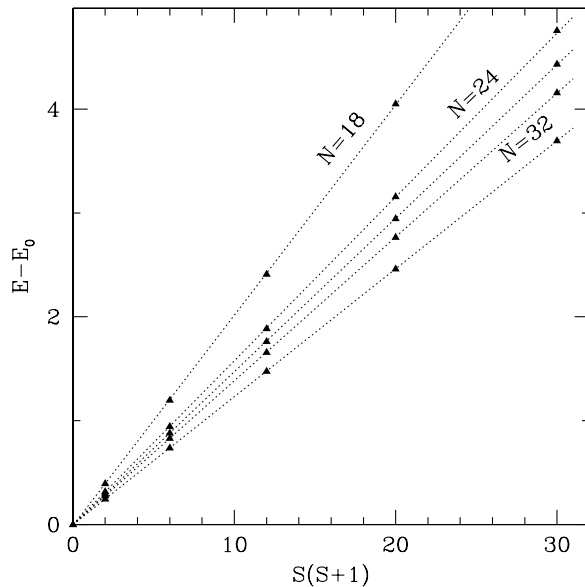


Figure 1.5: AF Heisenberg model on the honeycomb lattice, scaling of the QDJS with S and N for $N = 18, 24, 26, 28, 32$ (taken from ref. [18]).

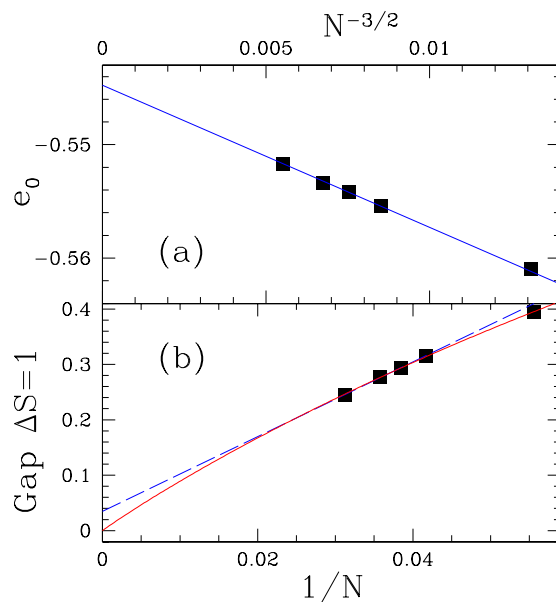


Figure 1.6: AF Heisenberg model on the honeycomb lattice, (a) energy per site e_0 versus $N^{-3/2}$ (b) spin-gap: The dashed line is a linear fit in $1/N$: for the sizes of interest the restriction to the leading term of the finite size expansion is insufficient. The full line is a fit to eq. [12, 14]: $\Delta(N) = \frac{1}{4\chi N} (1 - \beta \frac{c}{\rho\sqrt{N}}) + \mathcal{O}(\frac{1}{N^2})$ where χ is the spin susceptibility, c is the spin-wave velocity, ρ the spin stiffness and β is a number of order one (taken from ref. [18]).

1.3 When the adiabatic continuation scenario fails

1.3.1 Order from disorder selection

Thermal Order by Disorder selection in classical models

The concept of “order by disorder” was introduced in 1980 by Villain and co-workers[29] in the study of the fully frustrated Ising model on the square lattice.¹⁰ At $T = 0$ this model is disordered, with a residual entropy per spin $S_0 = \frac{1}{\sqrt{N}} \ln 2$. Thermal fluctuations select ordered ferrimagnetic configurations, whence the name of ”order by disorder” or ”order from disorder”.

During the nineties, several authors have studied a somewhat less drastic problem in classical frustrated vector models : it is the selection of a special kind of long range order among a larger family of ordered solutions classically degenerate at $T=0$ [30, 31, 32, 33, 34, 35, 36]. In the classical models, the selection by thermal fluctuations of the simplest order, is due to a larger density of low lying excitations around these solutions, whence an increased Boltzmann weight of the corresponding domains of phase space and a thermal (entropic) selection of order.

$T = 0$ order from disorder selection in quantum systems

A large density of low lying excitations also explains the selection of specific spin ground-states when going from the $T = 0$ classical vectorial spin models to their quantum counterpart. Let us consider the example of the $J_1 - J_2$ model on the triangular lattice. This Hamiltonian reads:

$$\mathcal{H} = 2J_1 \sum_{\langle i,j \rangle} \mathbf{S}_i \cdot \mathbf{S}_j + 2J_2 \sum_{\langle\langle i,k \rangle\rangle} \mathbf{S}_i \cdot \mathbf{S}_k \quad (1.24)$$

where J_1 and $J_2 = \alpha J_1$ are positive and the first and second sums run on the first and second neighbors, respectively. For classical spins [34], and

¹⁰In this model the next neighbor couplings along all the rows are ferromagnetic as well as those on the odd columns (named A in the following). The couplings on the even columns (named B) are antiferromagnetic. It is assumed that

$$0 < |J_{AB}| < J_{BB} < |J_{AA}|. \quad (1.23)$$

The ground-states of this model have A columns (resp B) ferromagnetically (resp. antiferromagnetically) ordered. For a system with a number of sites $N = 0 \pmod{4}$, the degeneracy of this ground-state is $2^{\sqrt{N}}$, its entropy per spin $S_0 = \frac{1}{\sqrt{N}} \ln 2$ is negligible in the thermodynamic limit. At $T = 0$ the ground-state has no average magnetization and is disordered. The picture changes when thermal fluctuations are introduced: it is readily seen that a B chain sandwiched between two A chains with parallel spins has lower excitations than a B chain sandwiched between two A chains with anti-parallel spins. This gives a larger Boltzmann weight to the ferrimagnetically ordered system. Villain and co-workers have been able to show exactly that the system is indeed ferrimagnetic at low T . They were equally able to show that site dilution (introducing non magnetic species) was in a certain domain of composition and temperature able to select the same ordered pattern, whence the name of “order by disorder”.

$1/8 < \alpha < 1$, the competing interactions leads to a continuous degeneracy of the ground-state described in Fig. 1.7. The study of the excitations of these various ground-states, shows a larger density of low lying excitations around the collinear 2-sublattice solutions. This property is the signature of a weaker restoring force toward this configuration (larger well width in phase space). Insofar as the semi-classical spin-wave approach is valid, this implies that the zero point quantum energy $\sum_{\mathbf{q} \in BZ^*} \frac{\omega_{\mathbf{q}}}{2}$ of Eq. 1.21 is smaller for this solution, which will thus be energetically selected by “quantum” fluctuations (for more details see the original papers by Chubukov and Jolicoeur [35] and Korshunov [36], Deutscher and Everts [37]).

Lecheminant *et al.* have given a direct illustration of the partial restoration of symmetry through the effects of quantum fluctuations on the Anderson tower of states [38]. The 4-sublattice Néel order is embedded in an Anderson tower with a multiplicity of order $\mathcal{O}(N^4)$ called $\{^4\tilde{E}\}$. These levels appears to be the low lying levels on the exact spectra of small samples (see the spectrum of the $N = 16$ spins sample in Fig. 1.8). But with the increase of the sample size, quantum fluctuations with longer wave-length favor the special set of levels embodying the 2-sublattice Néel order $\{^2\tilde{E}\}$ (bars in Fig. 1.9). The other levels evaporate gradually and don’t collapse to the macroscopic ground-state in the thermodynamic limit.


The selection of order is, in this case, much less drastic than in the original problem of Villain. It amounts essentially in an enlarging of the symmetry of the classical ground-state through quantum fluctuations. As it has been underlined previously such a problem is readily accessible to spin-waves calculations. We will now move to more drastic enlargements of the ground-state symmetry through quantum fluctuations, which can no more be tackled by spin-wave calculations.

1.3.2 A partial restoration of the $SU(2)$ symmetry by quantum fluctuations: the p-nematic magnet

Interplay of frustration and quantum fluctuations may lead to more surprising quantum ground-state.

The ring exchange model

The following example is drawn from a work by A. Läuchli *et al.*[39]. The $SU(2)$ invariant Hamiltonian involves a first neighbor Heisenberg term and cyclic ring exchange on the plaquettes of a square lattice:

$$H = K \sum_{\square} (P_{1\dots 4} + h.c) + J \sum_{\langle ij \rangle} \mathbf{S}_i \cdot \mathbf{S}_j \quad (1.25)$$


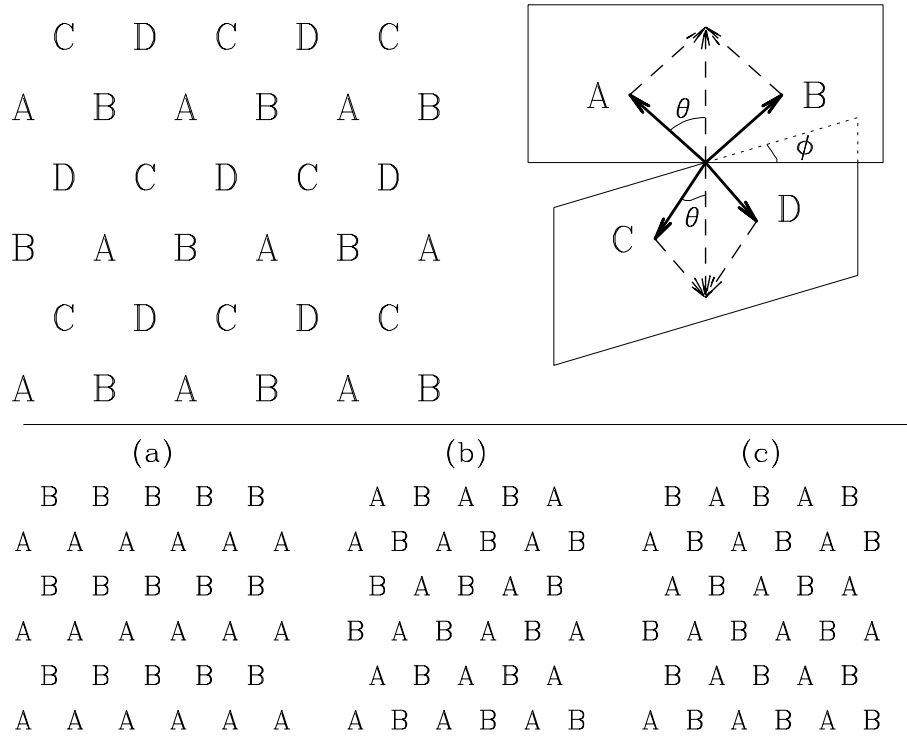


Figure 1.7: Top: 4-sublattice classical ground-state. Spins in the sublattices A and B , as well as spins in C and D , make an angle 2θ . The plane of the spins of A and B makes an angle ϕ with the plane of the spins of C and D . Bottom: the collinear solutions with the three possible arrangements (in this case, classical spins in sublattices A and B are antiparallel).

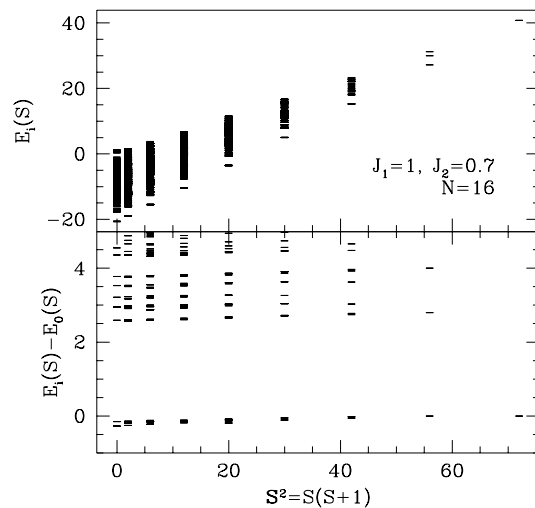


Figure 1.8: Top: spectrum of $J_1 - J_2$ model on the triangular lattice for the $N = 16$ sample. Bottom: zoom on the difference between the exact spectrum and the energies $E_0(S)$ of the low lying levels of the toy model associated to the present problem (see Lecheminant [38]). The ground-state multiplicity $\{^4\tilde{E}\}$ is well separated from the magnons.

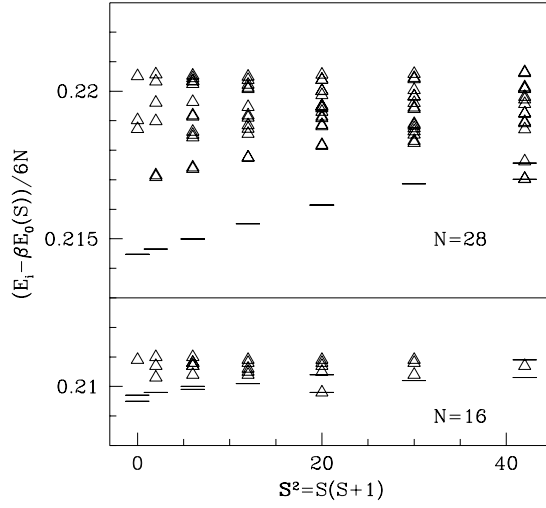


Figure 1.9: Zooms on the $N = 16$ and $N = 28$ Anderson tower of states of the $J_1 - J_2$ model on the triangular lattice (after Lecheminant [38]). A global contribution $\propto E_0(S)$ is subtracted from the exact spectrum. The bars represent eigenstates which belong both to $\{\tilde{E}^2\}$ and $\{\tilde{E}^4\}$. The triangles indicate states which belong to $\{\tilde{E}^4\}$ but not to $\{\tilde{E}^2\}$. With increasing sizes, the subset $\{\tilde{E}^2\}$ is stabilized and separates from the pure 4-sublattice order. For $N = 28$ the two states of $\{\tilde{E}^2\}$ with even S are quasi degenerate and cannot be distinguished at the scale of the figure.

$P_{1\dots 4}$ is the cyclic permutation of the 4 spins sitting around a square plaquette, and the various sums run respectively on the plaquettes and bonds of the lattice. Expression of the 4-spin permutation in terms of spin operators leads to:

$$H = 4K \sum_{\square} [(\mathbf{S}_1 \cdot \mathbf{S}_2)(\mathbf{S}_3 \cdot \mathbf{S}_4) + (\mathbf{S}_1 \cdot \mathbf{S}_4)(\mathbf{S}_2 \cdot \mathbf{S}_3) - (\mathbf{S}_1 \cdot \mathbf{S}_3)(\mathbf{S}_2 \cdot \mathbf{S}_4)] \quad (1.26)$$

$$+ (J + 2K) \sum_{\text{---}} \mathbf{S}_i \cdot \mathbf{S}_j + K \sum_{\text{---}} \mathbf{S}_i \cdot \mathbf{S}_j + (KN)/4.$$

For $J^{eff} = J + 2K = 0$, the physics of the quartic model is tightly related to the physics of the vectorial chirality on the square plaquettes. The vectorial chirality around a square plaquette is defined as:

$$\mathcal{C} = \mathbf{S}_1 \wedge \mathbf{S}_2 + \mathbf{S}_2 \wedge \mathbf{S}_3 + \mathbf{S}_3 \wedge \mathbf{S}_4 + \mathbf{S}_4 \wedge \mathbf{S}_1 \quad (1.27)$$

and it square reads:

$$\mathcal{C}^2 = -2 [(\mathbf{S}_1 \cdot \mathbf{S}_2)(\mathbf{S}_3 \cdot \mathbf{S}_4) + (\mathbf{S}_1 \cdot \mathbf{S}_4)(\mathbf{S}_2 \cdot \mathbf{S}_3) - 2(\mathbf{S}_1 \cdot \mathbf{S}_3)(\mathbf{S}_2 \cdot \mathbf{S}_4)] \quad (1.28)$$

$$- \frac{1}{2} [\mathbf{S}_1 \cdot \mathbf{S}_2 + \mathbf{S}_2 \cdot \mathbf{S}_3 + \mathbf{S}_3 \cdot \mathbf{S}_4 + \mathbf{S}_4 \cdot \mathbf{S}_1] - 2 [\mathbf{S}_1 \cdot \mathbf{S}_3 + \mathbf{S}_2 \cdot \mathbf{S}_4] + \frac{3}{2}.$$

The full hamiltonian (Eq.1.26) can be written as:

$$\mathcal{H} = -2K \sum_{\square} \mathcal{C}^2 + V \quad (1.29)$$

where the perturbation V is:

$$V = +4K \sum_{\square} (\mathbf{S}_1 \cdot \mathbf{S}_3)(\mathbf{S}_2 \cdot \mathbf{S}_4) + 3K \sum_{\text{---}} \mathbf{S}_i \cdot \mathbf{S}_j - 2K \sum_{\text{---}} \mathbf{S}_i \cdot \mathbf{S}_j + 13KN/4 \quad (1.30)$$

Classical phase diagram

The maximization of the vectorial chirality leads in the classical limit to an orthogonal state: i.e. a state with 4 sublattices, planar long range order and orthogonal spins on neighboring sites. The orthogonal state is the classical ground-state of Eq. 1.26 for $J = -2K$. When J moves away from the value $-2K$, J^{eff} frustrates the orthogonal state by introducing an effective ferromagnetic second neighbor interaction. For a large enough negative J^{eff} , the classical system is driven to the ferromagnetic phase, while an antiferromagnetic J^{eff} drives it to the standard (π, π) Néel phase.

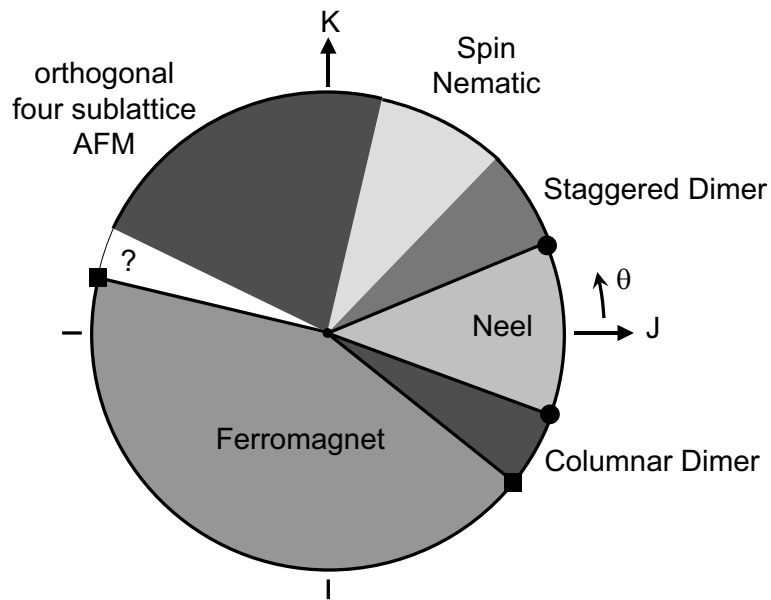


Figure 1.10: Phase diagram of the $K - J$ ring exchange model on the square lattice, from Läuchli *et al.*[39]. In the range of parameters in white, (with a questionmark), Shannon *et al.*[40] have found an $SU(2)$ symmetry breaking n-nematic phase.

Quantum phase diagram

The orthogonal state is also the quantum ground-state of Eq. 1.26 for $J = -2K$. But action of perturbations leads to intermediate phases before recovering either the ferromagnetic phase, or the (π, π) Néel phase (see phase diagram in Fig. 1.10). We will first discuss the p-nematic phase obtained by destabilization of the 4 sub-lattice order by an antiferromagnetic first neighbor interaction.

The p-nematic phase

In this phase there is no long range order in spin-spin correlations, but there is (π, π) long range order in the vectorial chirality \mathcal{C} defined in Eq.1.27. The magnetization per spin is zero, but the current of spin around the square plaquettes remains ordered. This phase takes its name from the nature of the order parameter, which is no more a vector (an operator linear in spin) but a tensor (quartic in spin).¹¹ Such an ordered phase

- breaks the spin rotational symmetry of the original hamiltonian: in the nematic state, the spins are disordered but they live in a plane. Its first excitations are Goldstone modes: pseudo-spin waves which only differ from the usual ones by subtle selection rules (see next item).
- It also breaks the inversion symmetry (as a simple magnetic moment) but, contrary to simple magnetic moments, it does not break time reversal symmetry.

All these properties can be immediately disclosed from the analysis of the spectra and of their finite size scaling displayed in Fig.1.11. Contrary to the 4-sublattice order which totally breaks the spin rotational symmetry, in the nematic state the rotational symmetry in the spin plane is unbroken ($U(1)$ symmetry is conserved). Evolution from the 4-sublattice phase to the vectorial chiral phase corresponds to a partial restoration of $SU(2)$ symmetry. This enlargement of the symmetry is accompanied by a decrease of the number of Goldstone modes from 3 to 2 (see [39] for details)

The scenario describing the evolution from the orthogonal 4-sublattice order to this nematic state can be described in simple words as follows. The J^{eff} Heisenberg term frustrates the 4-sublattice order. Associated to the disordering effect of quantum fluctuations it tends to kill the 4-sublattice macroscopic magnetic moment, but the quartic term which remains dominant protect the vectorial chirality. By the fact, the quantum fluctuations

¹¹To be more precise it is an irreducible rank-1 tensor, that is a pseudo vector. This denomination nematic was introduced by Andreev and Grishchuk [41] and further used by Chandra and Coleman[42]. In the n-nematic studied below the order parameter is the irreducible symmetric tensor of rank-2: the order parameter is a director, a symmetry encountered in liquid crystals.

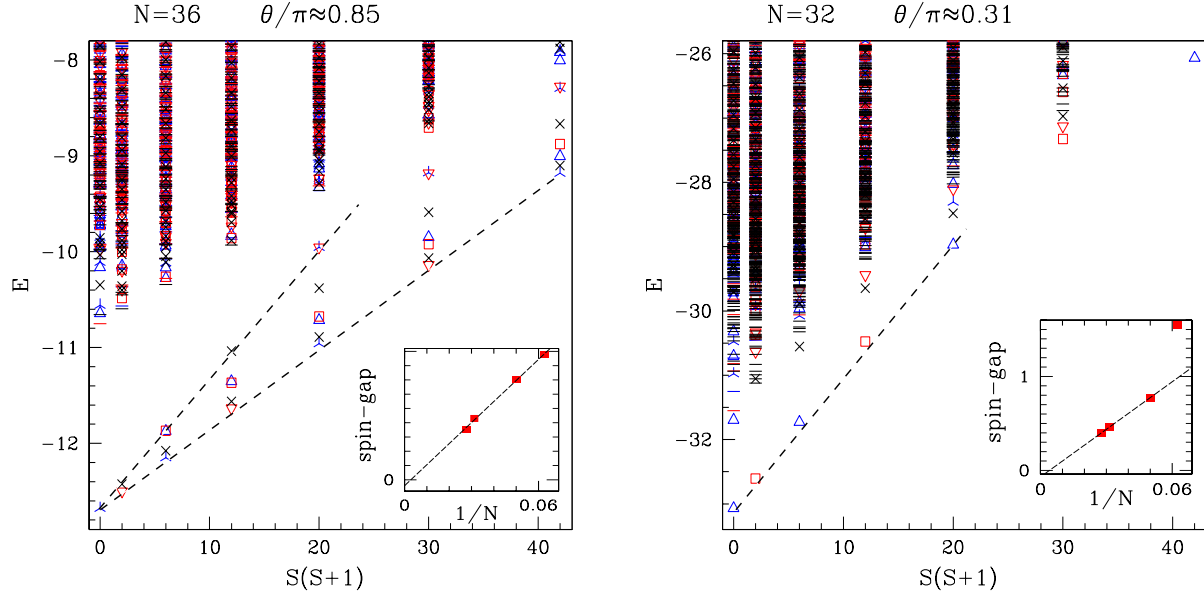


Figure 1.11: Low lying levels of the exact spectra of the orthogonal 4-sublattice Néel state ($\theta = 0.85\pi$) (left) and of the nematic phase $\theta = 0.31\pi$ (right) versus $S(S+1)$ the eigenvalue of the square of the total spin. The different symbols are associated to the different IRs of the rotation group D_4 : upright triangle, A_1 , square, A_2 , downwards triangle, B_1 , tripod, B_2 , cross, E . The levels between the two dashed lines in the left figure are the levels of the Anderson tower of states explicated in ref. [39]. There are $2S+1$ distinct levels for each value of the total spin S , because of the full symmetry breaking of $SU(2)$. In the nematic phase on the contrary $SU(2)$ is only broken to $U(1)$, and there is only one (degenerate) S level in the Anderson tower. In the insets, one can see that in both phases, these levels collapse as in $1/N$ to the ground-state: supporting the continuous symmetry breaking schemes.

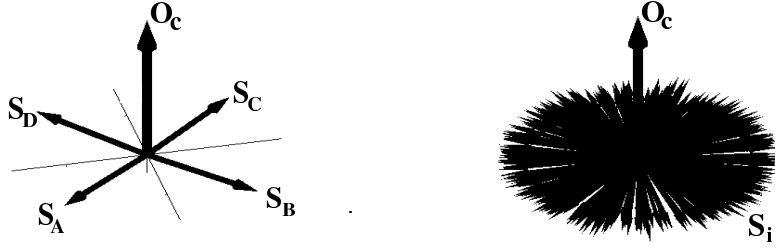


Figure 1.12: From the orthogonal 4-sublattice Néel state (left) to the nematic phase (right).

increase more rapidly in the plane of spins than perpendicular to it, and the plane of spins remains locked, albeit the spin disorder perpendicular to the vectorial chirality (see the cartoon given in Fig.1.12).

It may be noticed that usual spin-approaches fail to disclose this symmetry breaking phase.

Further increase of the antiferromagnetic frustration overcomes the protecting effect of the quartic term on the vectorial chirality, the plane of spins unlocks under the conjugate effects of frustration and quantum fluctuations and the system is driven to a fully $SU(2)$ invariant staggered VBC studied in the next section and chapter.

The n-nematic phase

The transition from the ferromagnetic phase to the 4-sublattice Néel phase also involves intermediate phases in the quantum case. From the ferromagnetic phase and under the influence of the quartic term which frustrates the ferromagnet the system passes through an $SU(2)$ symmetry breaking phase without spin order on any site. The order parameter is a director, that is a symmetric tensor of rank 2 build from two neighboring spins. This phase breaks $SU(2)$ and its first excitations are modes associated to $\Delta S = 2$ excitations (see [40] for more details).

1.3.3 Full destruction of the semi-classical phases by quantum fluctuations: VBC and RVB phases

As shown in Fig. 1.10, the two $SU(2)$ symmetry breaking phases the chiral p-nematic phase and the (π, π) Néel phase are separated by a phase that we call a **Valence Bond Crystal**. In this phase there is no long range order in

spin¹². But there is (π, π) **long range order in the pattern of singlet bonds**: whence the name of Valence Bond Crystal. This phase does not break $SU(2)$ symmetry, but breaks the lattice symmetry (both translation and C_4). Its first excitations are gapped $\Delta S = 1$ modes. Valence Bond crystals will be the subject of the next lecture.

Valence Bond Crystals are sometimes classified as spin liquids inasmuch as there is no long range order in spins. We use exclusively the name of Spin Liquids, or better of **Resonating Valence Bond Spin Liquids (RVB in the following) for phases which do not break any local symmetry.**

¹³

Resonating Valence Bond Spin Liquids will be the subject of the last lecture.

1.3.4 Some omissions, and relevant refs.

A few points of importance have been omitted in this first chapter.

First the question of order by disorder in systems where the degeneracy of the classical ground-state is so large that there is a residual entropy per spin at $T = 0$. It is the case of the Heisenberg model on the kagome or pyrochlore lattices. The answer is probably not unique (as will be seen in next chapter where we study the model on the 2-dimensional or checker board lattice), and probably depends on the value of the quantum spin in a unit cell of the lattice. This point has been extensively analyzed in ([47]). To our knowledge nothing radically new appears on the subject since that review. This remains a very difficult issue.

The second point of importance concerns the nature of the quantum phase transitions between these different phases. Senthil, Vishwanath, Balents, Sachdev and Fisher have recently proposed a new scenario to describe the excitations at the quantum critical point between the collinear Néel order and the Valence Bond Crystal[48]. In this scenario, beyond the Landau paradigm, unconfined spin-1/2 excitations become the dominant gapless excitations. The above mentioned ring exchange model on the square lattice would be an excellent model to check this field theoretical approach. To our knowledge nothing has been done up to now in this direction.

....

¹²nor in any tensorial order parameter of rank non zero built with the original spins

¹³It has been advocated, by Read, Sachdev and collaborators[43, 44, 45, 46] on the basis of the study of quantum fluctuations around mean field saddle points solutions of large N models ($Sp(N)$) that destruction of collinear order should systematically give rise to these VBC phases, whereas the pure Resonating Valence Bond Spin Liquids (RVB in the following), which do not break any local symmetry, were to be expected in quantum models where the classical counterparts have non collinear order. Up to now exact diagonalizations of $SU(2)$ models up to now strongly support this assumption. For more details, see the above-mentioned refs. The review by Misguich *et al.* [47] gives a quick summary of the.

1.4 Complement-1 A simple conceptual approach of the translational symmetry breaking in a solid

For a while we exclude any calculations and just rely on very simple and basic concepts of condensed matter physics and quantum mechanics to derive the “necessary” structure of the spectra of ordered condensed matter in finite size samples. For the sake of simplicity, we begin with the problem of the solid phase. We successively expose the fundamental classical hypothesis underlying the theory of solids. Quantization of this picture enlightens the translational symmetry breaking mechanism and finite size effects give a new light on the absence of solid order in 1-dimensional physics.

1.4.1 An essential classical hypothesis

Let us consider a finite sample of solid with N atoms of individual mass m . The Hamiltonian of this piece of solid contains a kinetic energy term and an interaction term $U(\mathbf{r}_i - \mathbf{r}_j)$, which essentially depends on distances between the N atoms, and is translation invariant. Nevertheless any piece of solid in nature breaks translational symmetry!

The first step in the description in classical phase space of the dynamics of this object with $2dN$ degrees of freedom, consists in sorting these variables in two sets:

- the center of mass variables: $\mathbf{R}_{c.o.m}$ and $\mathbf{P}_{c.o.m}$, the dynamics of which is a pure kinetic term \mathcal{K} :

$$\mathcal{K} = \frac{\mathbf{P}^2}{2Nm} \quad (1.31)$$

- and the $2d(N - 1)$ internal variables, which obey a dynamic with interactions:

$$\mathcal{H}_{int} = \sum_{i \in [1, \dots, N]} \left[\frac{\mathbf{p}_i^2}{2m} + U(\mathbf{r}_i - \mathbf{r}_j) \right] \quad (1.32)$$

Then invoking the inertia principle, the analysis of the problem focuses on the Galilean frame, where the center of mass is at rest. In this frame, the internal excitations are analyzed in first approximation as modes of vibrations: the phonons, which present a dispersion law linear in \mathbf{k} for small wave vectors \mathbf{k} .

In so doing, an **essential dichotomy** is introduced between the global variable and its dynamics on one hand and the internal excitations on the other: this dichotomy is at the basis of the concept of an ordered phase [49]. A technical asymmetry is also introduced in the treatment of the dynamics of these two sets of variables: the center of mass dynamics is described in

a classical framework which explicitly breaks the translation invariance of the total Hamiltonian of the solid $\mathcal{K} + \mathcal{H}_{int}$. On the other hand the internal excitations are looked at in a translationally invariant (eventually quantum) point of view. This point of view may seem inconsistent in particular when looking at a finite sized, eventually small, piece of solid.

Taking as a definition of the solid phase the essential distinction between the global variable and the internal ones, we will show that the technical asymmetry in the treatment of these variables can be easily overcome, thus explaining both the localization of a piece of solid in real space, and the influence of space dimensionality on the definition of this solid.

1.4.2 Quantization of the classical approach, finite size spectra, thermodynamic limit and translational symmetry breaking

In order not to break artificially the translational symmetry of the problem we consider a solid with periodic boundary conditions.

If we take for granted that it is legitimate to disconnect the center of mass dynamics from the internal excitations we may consider a solid at $T = 0$ with no internal excitations: the vacuum of phonons that we will write $|0\rangle$.

The translationally invariant eigen-states of \mathcal{K} are the plane waves with wave-vectors \mathbf{k} where $k_{x,y,z} = n_{x,y,z} \frac{2\pi}{L}$, L is the linear length of the sample and $n_{x,y,z}$ non zero integers. Their eigen-values are of the general form:

$$\frac{\hbar^2 \mathbf{k}^2}{2mN}. \quad (1.33)$$

The total energy of the solid in these states is thus of the form:

$$E_0(k) = \frac{\hbar^2 \mathbf{k}^2}{2mN} + E_g, \quad (1.34)$$

where E_g is a constant measuring the zero point energy of the internal degrees of freedom. These eigen-states are shown in Fig. 1.13 connected by the red continuous line noted $|0\rangle$.

In order to localize the center of mass it is necessary to form a wave-packet with eigen-states of \mathcal{K} showing a large distribution of wave-vectors \mathbf{k} : the largest the \mathbf{k} -distribution be, the better the localization of the center of mass. Such a wave-packet is non stationary for a finite size, but its evolution rate goes to zero as $\mathcal{O}(1/N)$. Localization of the center of mass is thus a costless operation in the thermodynamic limit.

Let us look now to the first excitation of the solid with one phonon of wave vector $\mathbf{k}_{min} = 2\pi/L$. This state can typically be written in a symmetry

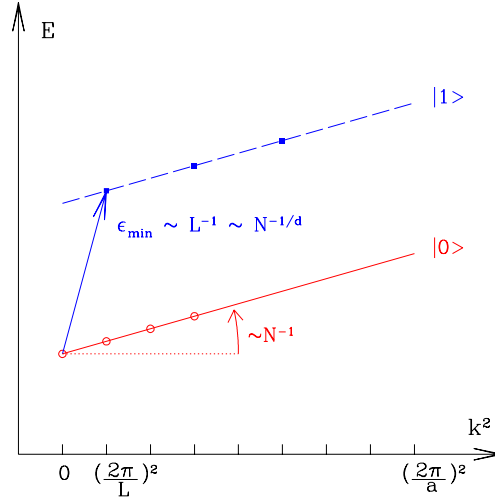


Figure 1.13: Typical spectrum of a finite size solid. The tower of eigen-levels joined by the continuous line and noted $|0\rangle$ is the Anderson tower of states needed to form a symmetry breaking vacuum of phonons of the solid: such a state is non stationary on a finite size sample. The second set $|1\rangle$ (dashed line) is associated with the lowest phonon.

breaking picture as:

$$|1\rangle = \exp\left(\sum_j i\mathbf{k}_{min}\cdot\mathbf{r}_j\right) |0\rangle \quad (1.35)$$

It thus involves a linear superposition of eigenstates of $\mathcal{K} + \mathcal{H}_{int}$ with a distribution of wave vectors displaced by \mathbf{k}_{min} with respect to the distribution of the localized ground-state $|0\rangle$. This second set of excitations is displayed in Fig. 1.13 with a dashed line noted $|1\rangle$ joining the different eigen-states. The softest phonon has an energy proportional to $k_{min} \propto L^{-1} \propto N^{-1/d}$ which should be added to the ground-state energy (1.34) giving eigen-states with eigen-energies:

$$E_1(k) = \frac{\hbar^2\mathbf{k}^2}{2mN} + E_g + \hbar ck, \quad (1.36)$$

where c is the sound velocity. Due to the structure of equation (1.36) the line joining the different translation invariant states of this soft phonon is parallel to the ground-state line $|0\rangle$. This explains the supposed-to-be structure of the low lying levels of a finite size solid exhibited in Fig. 1.13.

1.4.3 Thermodynamic limit, stability of the solid and self-consistency of the approach

The consistency of the semi-classical picture implies that the localization of the center of mass could be done whatever the degree of excitations of phonons: looking to the finite size effects this appears to be the case if the dimension of space is larger or equal to 2. In these situations, for large enough sizes there appears two different scales of energy: the Anderson tower of states of the ground-state collapses as N^{-1} to the absolute ground-state whereas the softest phonon collapses on the ground-state only as $N^{-1/d}$. In this limit, the dichotomy between the dynamics of the global variable and the internal variables is totally justified. On the other hand in 1 dimension it is quantum mechanically inconsistent to separate global degrees of freedom from internal ones: these two types of variables having dynamics that cannot be disentangled.

1.5 Complement-2: $SU(2)$ symmetry breaking in the Néel antiferromagnet

Let us now develop the analogy between the solid states and the antiferromagnetic ones.

- The global variables of the solid are $\mathbf{R}_{c.o.m}$ and the conjugate variable $\mathbf{P}_{c.o.m}$. In the collinear antiferromagnetic case the global variables of position of the magnet are the two Euler angles (θ, ϕ) allowing to point the direction of the sublattice magnetization in spin space. Their conjugate variable is the total spin operator \mathbf{S} .
- The free motion of the center of mass is governed by the Hamiltonian \mathcal{K} (the quadratic form of this kinetic energy being related to the homogeneity of space). By analogy we expect the kinetic energy term describing the free precession of the sublattice magnetization to be of the form: $\mathcal{K}_{spin} = \mathbf{S}_{tot}^2/2van$ ¹⁴. In such a point of view the constant a is just a multiplicative term: we know from other sources (fluctuation dissipation theorem or macroscopic approach of the magnet) that this is up to a constant the homogeneous spin susceptibility.
- The eigen-states describing the free precession of the order parameter in the vacuum of magnons are thus states with total spin S (ranging

¹⁴A three sublattice Néel order has a more complicated order parameter: the three Euler angles are needed to localize the 3 sublattice magnetizations: and the macroscopic object is no more a rigid rotator as in the case of the collinear Néel order but a (symmetric) top. There is in that last case an extra internal spin kinetic energy term and as already explained in the previous section the Hilbert space of the problem is larger. See ref. [1] for example or the quantum mechanical theory of symmetric top molecules.

from 0 to $N/2$), and eigen-energies:

$$E_0(S(S+1)) = \frac{\hbar^2 S(S+1)}{2\chi N} + E_g \quad (1.37)$$

They form the set $|0\rangle$ of Fig. 1.2. By forming a wave-packet out of this set one can localize the direction of the sublattice magnetization and break $SU(2)$ symmetry.

- The discussion of the first excitations above the vacuum of magnon completely parallelizes that of the phonons excitations (same dispersion law and same finite size scaling law). The eigen-energies of the states embedded in the softest magnon (referred as $|1\rangle$ in Fig. 1.2) are thus of the form:

$$E_1(S(S+1)) = \frac{\hbar^2 S(S+1)}{2\chi N} + E_g + \hbar c_s k_{min} \quad (1.38)$$

where c_s is the spin wave velocity.

- The possibility of a spin rotational symmetry breaking at the thermodynamic limit is embodied in the finite size behavior of the low lying levels of the spectra (Fig. 1.2). In dimension $d \geq 2$ the eigen-states of the sets $|0\rangle$ (resp. $|1\rangle$) collapse on their $S = S_{min}$ component as $\mathcal{O}(N^{-1})$, more rapidly than the decrease in energy of the softest magnon which is $\mathcal{O}(N^{-1/2})$. In dimension 2 and higher, the $SU(2)$ breaking mechanism prevails on the formation of magnon excitations justifying the classical approach and the dichotomy between global classical variables and internal excitations.
- These finite size scalings of the Anderson tower of states and of the true physical excitations (the magnons) give a new light on the Mermin Wagner theorem which denies the existence of Néel long range order in 1 dimensional magnets.

Chapter 2

Valence Bond Crystals

In this chapter we will concentrate on situations where there is no $SU(2)$ symmetry breaking, no long range order in spin-spins correlations (which decrease exponentially with distance), BUT **long range order in dimer or larger $S = 0$ units**: we will call these phases generically **Valence Bond Crystals** (VBC).

Except at a quantum critical point, all excitations of a VBC are gapped.

Depending on the lattice geometry, such a wave function can spontaneously break some lattice symmetry (*spontaneous VBC*) or can remain fully symmetric (*explicit VBC*).

2.1 1-dimensional VBC

Such ground-states are well known in 1-dimensional problems as for example in the spin-1/2 A.F. $J_1 - J_2$ model:

$$\mathcal{H} = J_1 \sum_{\langle ij \rangle} \mathbf{S}_i \cdot \mathbf{S}_j + J_2 \sum_{\langle\langle ij \rangle\rangle} \mathbf{S}_i \cdot \mathbf{S}_j \quad (2.1)$$

where the first (resp. second) sums run on first (resp. second) neighbors. In 1-d, for $J_2/J_1 > 0.24$, the ground-state is dimerized and there is a gap to the first excitations: this is the simplest case of a VBC. In fact for $J_2/J_1 = 0.5$ (Majumdar and Ghosh point) the doubly degenerate ground-states are exact product of valence bonds:[50, 17]

$$|MG_{\pm}\rangle = \prod_{n=1}^{N/2} |(2n, 2n \pm 1)\rangle. \quad (2.2)$$

Here and in the following we call valence bond a pair of spins in a singlet state, and note it:

$$|(i, j)\rangle = \frac{1}{\sqrt{2}} \{ |i, +\rangle |j, -\rangle - |i, -\rangle |j, +\rangle \}. \quad (2.3)$$

Other 1-D (the Heisenberg chain with alternate coupling) or quasi 1-D systems (ladders) also exhibit valence bond long range order and can be classified as VBC (see the revue by Lecheminant in the volume 'Frustrated Spin Systems (Diep editor) [51]).

First excitations are usually gapped, they are in general integer spin excitations appearing as modes, separated from a continuum of two-particle excitations. There are some exceptions: the $J_1 - J_2$ model where the excitations are scattering pairs of spin-1/2 solitons forming a continuum (this is quite specific of the 1-D system), or frustrated ladders [52], where excitations appear as a continuum of dynamical pairs of singlet or triplet domain walls.

2.2 A quick glance on two-dimensional VBC

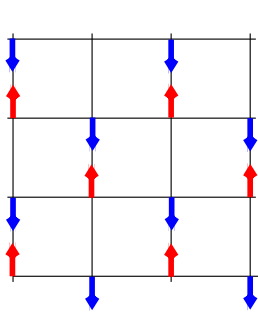
2.2.1 The $J_1 - J_2$ model on the square lattice

The more studied example and still the more debated! (For a more detailed approach see Misguich [47])

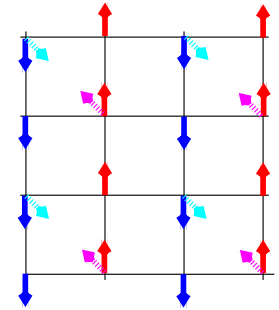
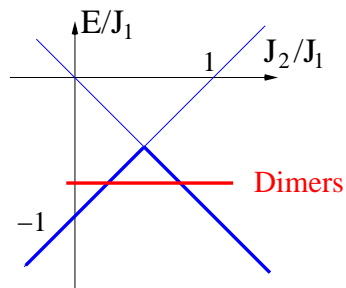
In a classical approach, the ground-state of Eq. (2.1) on a square lattice has a soft mode at (π, π) for $J_2/J_1 < 0.5$. At $J_2/J_1 = 0.5$, the (π, π) order is degenerate with 4-sublattice order and collinear $(\pi, 0)$ or $(0, \pi)$ order. For $J_2/J_1 > 0.5$, quantum fluctuations select the collinear $(\pi, 0)$ or $(0, \pi)$ order by the phenomenon of “order by disorder” (see Fig. 2.1).

In a naive approach, comparing the energies of classical Néel solutions to valence bond covering ones, we would conclude that any valence bond covering solution is more stable than any classical Néel order in a large range of parameters around $J_2/J_1 = 0.5$. In fact “quantum fluctuations” stabilize the Néel states and the window for an exotic phase is smaller than indicated in Fig. 2.1. The nature of the quantum phase(s) on the square lattice at $J_2/J_1 = 0.5$ is still hotly debated [53, 54, 55, 56, 57, 58]¹.

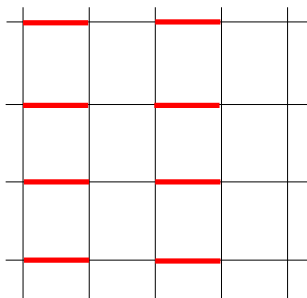
¹At this point of maximum frustration, Néel order is destroyed but the exact nature of the phase is uncertain: columnar order [53, 55], 4-spin plaquette order [54, 57] or RVB spin liquid [58]? In view of exact spectra for sizes up to N=36, it seems that the 4-spin S=0 plaquette order is the less plausible (because the $\mathbf{k} = (\pi, \pi)$ states necessary for the 2-fold symmetry breaking of this state is very high in the spectrum). We expect a 4-fold symmetry breaking in the columnar state as well as in the RVB state ([59] and refs. therein). The gaps from the ground-state to the plausible candidates for these 4-fold symmetry breakings are still very large in the N=36 sample. We are thus lead to conclude that the N=36 sample is too small to give informative issue on the dilemma: columnar state or RVB state. This strongly weakens the variational argument of ref. [58].



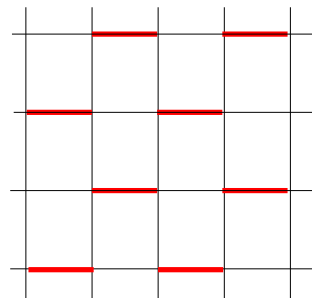
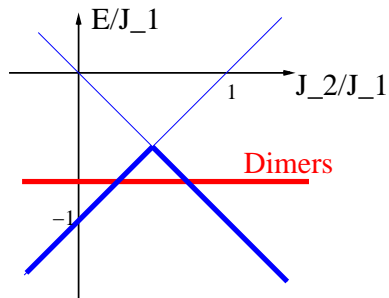
disorder
fluct.



Selection of order by
& Restoration of symmetry by



columnar VBC



staggered VBC

Figure 2.1: Schematization of different variational solutions of the $J_1 - J_2$ model on the square lattice

2.2.2 More consensual examples: from strong coupling solutions to explicit VBC

When the Hamiltonian has some inequivalent bonds and an integer spin in the unit cell (even number of spin- $\frac{1}{2}$ for instance)² the system can take full advantage of the strong bonds and minimize the effects of the frustrating ones.

The Shastry-Sutherland model and the 1/5 depleted square lattice are in this class. Two spin- $\frac{1}{2}$ experimental examples of 2D (explicit) VBC have recently attracted attention: CaV_4O_9 [60, 61, 62, 63, 64, 65] and $\text{SrCu}_2(\text{BO}_3)_2$ [66, 67, 68, 69, 70, 71, 72, 73, 74, 75]. See the original papers or [47] for more details.

In such cases the *explicit* VBC is the “natural” strong coupling solution. One can build a simple Hamiltonian in which the bonds which are not occupied by the singlet objects are turned off. The resulting model is a set of small decoupled clusters (dimers or larger plaquettes) and the ground-state is a trivial product of singlets. Importantly, this strong coupling limit has the same lattice symmetry as the original one. Going back to the original Hamiltonian *no quantum phase transition is encountered when going from the trivial singlet product up to the real interacting ground-state*.

2.2.3 Spontaneous VBC

In contrast to the previous example, there exist situations, where frustration makes regular pattern of singlet objects more favorable than other solutions but there is no unique elected position for the $2n$ -mers and a symmetry breaking must take place in order to form a VBC. This is what we call Spontaneous VBC. Models with an half-odd-integer spin in the unit cell cannot realize a VBC unless they *spontaneously* enlarge their unit cell.

The $J_1 - J_2$ model around $J_2 - J_1 \sim 0.5$ is the usual first example of spontaneous VBC. Fortunately there are other examples less difficult for theoreticians.

The two phases adjacent to the (π, π) Néel phase in the ring exchange model on the square lattice (studied in the previous chapter) are two good examples of Valence Bond Crystals, where the pattern of valence bonds is either columnar or staggered.

For fun, and further discussion of correlated issues, we will now describe in details a more exotic clear cut Valence Bond Crystal with a larger basic unit: the Heisenberg model on the checkerboard lattice [76, 22] (noted in the following HCKB).

²As it is the case in the alternate spin Peierls chain

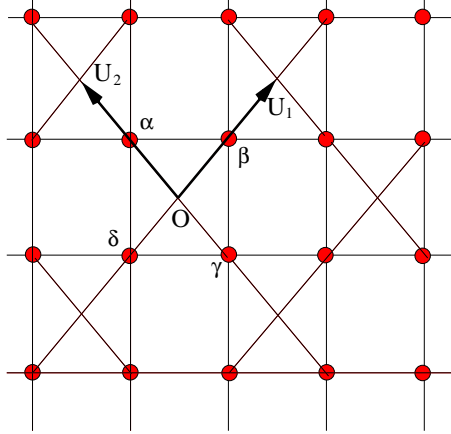


Figure 2.2: The checkerboard lattice: the spins sit at the vertices shown by bullets, all couplings are identical, $\mathbf{u}_1, \mathbf{u}_2$ are the unit vectors of the Bravais lattice.

2.3 The Heisenberg model on the checker-board lattice: an example of a Valence Bond Crystal

The checker-board lattice is made of corner sharing tetrahedrons, with all bonds equal: this is a 2-dimensional slice of a pyrochlore lattice. The underlying Bravais lattice is a square lattice and there are two spins per unit cell (Fig. 2.2).

2.3.1 Classical ground-states

The Heisenberg Hamiltonian on such a lattice is highly degenerate in the classical limit. Due to the special form of the lattice this Hamiltonian can be rewritten as the sum of the square of the total spin of corner sharing units α :

$$\mathcal{H} = J \sum_{(i,j) \text{ bonds}} \mathbf{S}_i \cdot \mathbf{S}_j \equiv \frac{J}{2} \sum_{\alpha \text{ units}} \mathbf{S}_\alpha^2 - \frac{NJ}{4}. \quad (2.4)$$

A classical ground-state is obtained whenever $\forall \alpha \mathbf{S}_\alpha = 0$. Such ground-states have a continuous local degeneracy and an energy $-(NJ)/4$. This is much higher than the valence bond covering energy, which is $-(3NJ)/8$. As we will see below, there is no memory of these classical solutions in the quantum ground-states and no selection of order out of disorder.

2.3.2 The Quantum HCKB model: Spin Gap

The first salient feature of the Heisenberg model on the checker-board lattice is the existence of a large spin gap (Fig. 2.3). This indicates that the ground-

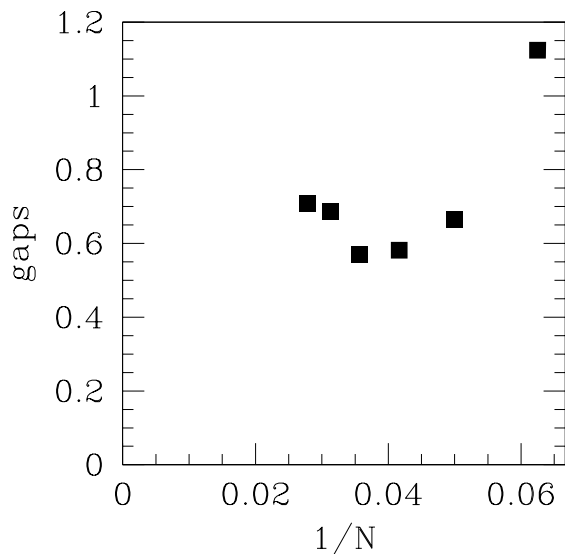


Figure 2.3: Gap between the absolute ground-state and the first S=1 excitation of the HCKB model versus sample sizes.

state does not break the $SU(2)$ symmetry of the Hamiltonian, and as a corollary we expect that the spin-spin correlations decrease exponentially to zero at large distance (which seems well verified, see ref. [22]).

2.3.3 Degeneracy of the ground-state and space symmetry breaking in the thermodynamic limit

The low lying levels of the spectra of the HCKB model in the singlet space are displayed in Fig. 2.4.

In this figure, one reads that the first excited singlet state very plausibly collapses to the absolute ground-state, whereas a finite gap to the third S=0 level (perhaps smaller than the spin gap) build on with sample size. This pleads in favor of a 2-fold degeneracy of the absolute ground-state in the thermodynamic limit.

The absolute ground-state is in the trivial representation of the lattice symmetry group. Its wave function is invariant in any translation and in any operation of D_4 (group of $\pi/2$ rotations around point O and axial symmetries with respect to axes \mathbf{u}_1 and \mathbf{u}_2). The S=0 excited state which collapses on it in the thermodynamic limit has a wave vector (π, π) , and is odd under $\pi/2$ rotations and axial symmetries. In the thermodynamic limit the 2-fold degenerate ground-state can thus exhibit a spontaneous symmetry breaking with a doubling of the unit cell.

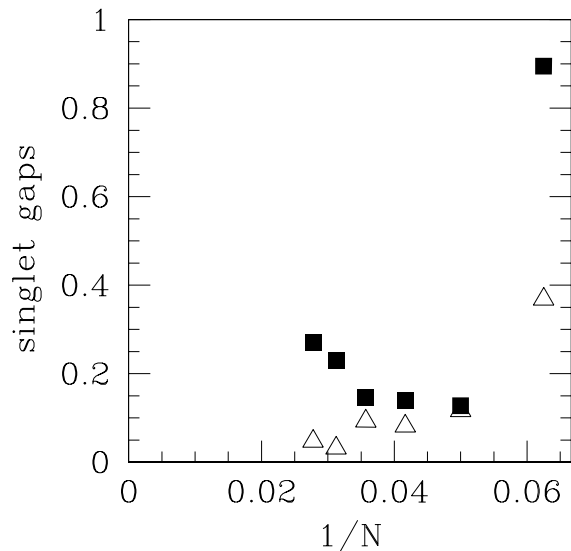


Figure 2.4: Gaps to the first (open up triangles) and second (black squares) level of the singlet sector. For the studied samples these two “excited” singlet levels are in the singlet-triplet gap (See Fig. 2.3).

Such a restricted symmetry breaking does not allow a columnar or staggered configuration of dimers: both of these states have at least a 4-fold degeneracy (Fig. 2.5). The simplest Valence Bond Crystals that allow

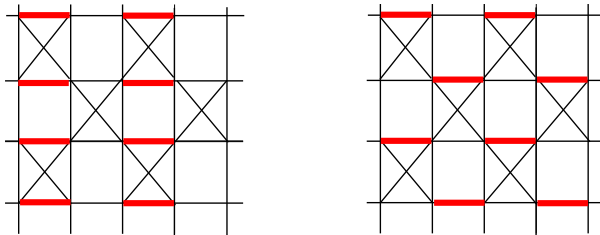


Figure 2.5: Columnar and staggered configuration of dimers (fat links) on the checkerboard lattice: such symmetry breaking configurations are 4-fold degenerate in the thermodynamic limit.

the above-mentioned symmetry breaking are described by product wave-functions of $S=0$ 4-spin plaquettes.

A further analysis of the space symmetries of the doublet ground-state done by Fouet and coworkers [22] shows that the basic unit of the g.-s. is a 4-spin $S=0$ plaquette sitting on void squares (B configuration of Fig. 2.6), with wave-function:

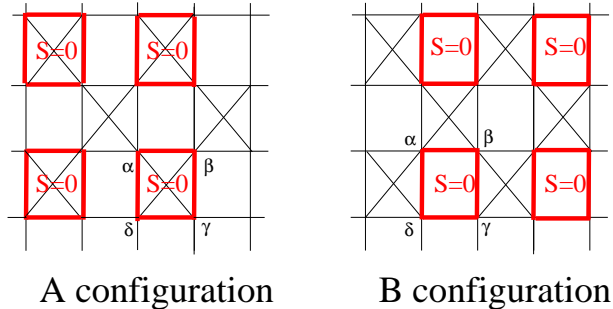


Figure 2.6: $S=0$ 4-spin plaquette valence-bond crystals on the checkerboard lattice: fat links indicate 4 spins involved in a singlet.

$$|\psi^+\rangle = |\alpha, \delta\rangle |\gamma, \beta\rangle + |\alpha, \beta\rangle |\gamma, \delta\rangle, \quad (2.5)$$

where $|\alpha, \gamma\rangle$ is the VB singlet state on sites α and γ :

$$|\alpha, \gamma\rangle = (|\alpha \uparrow, \gamma \downarrow\rangle - |\alpha \downarrow, \gamma \uparrow\rangle) / \sqrt{2}. \quad (2.6)$$

A simple remark could be done: the symmetric-plaquette state (Eq. 2.5) can be rewritten as the product of two triplets along the diagonals of the square. This configuration of spins is not energetically optimal on the squares with antiferromagnetic crossed links (A configuration) but is favored in B configuration. The variational energy *per spin* of the product wavefunction of ψ^+ - states in B configuration is $E_{var}(B^+) = -0.5^3$, whereas the exact energy *per spin* is $E_{ex} \sim -0.514 \pm 0.006$. The variational w-f is a very good approximation of the exact ground-state, as can be seen also on dimer-dimer and plaquette-plaquette correlations [22].

2.3.4 Excitations: raw data and qualitative description of the first excitations

Triplet excitations are gapped (gap of the order of 0.7) and very weakly dispersive. Singlet excitations too are gapped; they are much more dispersive than the triplet excitations and less energetic (gap of the order of 0.25). See Fig. 2.7.

There is a very simple variational description of the triplet excitations: let us consider the 4-spin plaquettes B of the ground-state. The $S=0$ ground-state is formed from the coupling of two triplets along the diagonals. There are four $S=1$ states on such a plaquette. The lowest $S=1$ excitation simply results from the $S=1$ coupling of the two diagonal triplets. The gap to this

³This is to be compared to the variational energy per spin of a pure dimer covering which is only: - 0.375

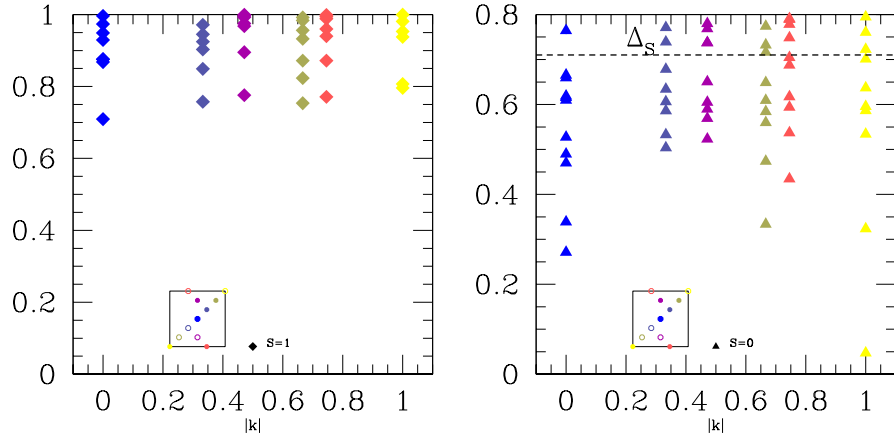


Figure 2.7: Left: Dispersion relations of the triplet (left) and singlet excitations (right) of the Heisenberg model on the checkerboard lattice versus $|\mathbf{k}|/|\mathbf{k}_0|$ with $\mathbf{k}_0 = (\pi, \pi)$. The insets show the correspondence between the colors of the symbols and the wave vectors in the Brillouin zone. The horizontal dashed line in the singlet excitations graph indicates the spin-gap.

variational excitation is 1. The Bloch waves built on such excitations are non dispersive. Up to a renormalization of the gap of the order of 33%, this picture appears as a good qualitative description of the true $S=1$ excitations of the HCKB model, which are massive, quasi localized excitations with an energy gap ~ 0.7 .

The singlet excitations are more intricate. Fouet *et al.* argue that these excitations may be associated to the reorganization of two symmetric ψ^+ states on two neighboring B positions. More precisely the excitation which promotes the two pairs of spins (α, δ) and (β, γ) into triplet states and then couples them in a singlet has a gap 1 with respect to the ground-state. To first order in a strong coupling expansion this excitation is non dispersive but it can acquire dispersion at higher order. The exact $S=0$ excitations are thus certainly a bit more extended and complex than this first order approximation. Berg *et al.* [77] have used a more sophisticated method (determination of an effective hamiltonian by a real space renormalisation method called CORE), and plead for domain walls between the two degenerate ground-states as the lowest excitations in the $S = 0$ sector.

This simple analysis of the singlet and triplet excitations of the HCKB model supports the idea that the excitations are simple integer spin modes or continua that could be observed in Raman, RPE, ESR or NMR spectra.

2.4 Valence Bond Solids

The concept was introduced by Affleck, Kennedy, Lieb and Tasaki (AKLT).[78, 79] The VBS wave-function can be constructed whenever the spin S on a site is a multiple of one half the coordination number z : $2S = 0 \pmod{z}$.

Let us consider the simplest case $2S = z$. In that case the local spin S can be seen as the symmetric combination of $2S$ (fictitious) spin- $\frac{1}{2}$. On each bond of the lattice one can make a singlet between two fictitious spins- $\frac{1}{2}$. Such a product of singlets does not belong to the physical Hilbert space of the original spin- S model but to a much larger space. The VBS wave-function is defined as the projection of the singlet-product state onto the physical space. This projection amounts to symmetrize (for all lattice sites) the wave-function with respect to the fictitious spins to force them into a physical spin- S state. By construction the VBS wave-function is a spin singlet and *breaks no lattice symmetry*. By extension we may say that a system is in a VBS *phase* if its ground-state can be adiabatically transformed into the VBS wave-function without crossing a phase transition.

Simple Hamiltonians with short ranged and $SU(2)$ -symmetric interactions for which the VBS is an exact ground-state can be constructed with the use of sum of projectors[78, 79]).

As the VBC, models in the VBS phase have a gap to all excitations⁴ but their wave-functions are slightly more complex and their order parameter is non-local. The order of VBS is associated to long-ranged singlet-singlet correlations in the *fictitious spins*. Expressing such observable in terms of the physical spins leads to a non-local quantity called *string order parameter*. [80, 81] Contrary to explicit VBC, VBS have **fractionalized degrees of freedom at the edges of the system with open boundary conditions**. These are simply associated to the unpaired fictitious spins. To our knowledge these properties have not been explored in quantum 2D systems.

The spin-1 Heisenberg or Haldane chain is the prototype of VBS in 1D. Such a state has a unique ground-state, a gap in the excitations and exponentially decreasing spin-spin and dimer-dimer correlations.

A spin- $\frac{3}{2}$ specific $SU(2)$ -invariant model on the honeycomb lattice[78, 79] is another example of 2D VBS. The spin-1 Heisenberg model on the kagome lattice was proposed to realize a VBS-like ground-state[82] in which singlets form on every hexagon without any spontaneous symmetry breaking (hexagonal singlet solid).⁵ A similar approach was carried out for the spin-1 py-

⁴This may however not always be true when the coordination number of the lattice is large.[78] In such cases the VBS wave-function is still a spin singlet but has long-ranged spin-spin correlations. We do not consider such cases here.

⁵Each kagome site belongs to two hexagons. Each physical spin-1 can be split into two spin- $\frac{1}{2}$, each of them being involved in the formation of a singlet on one neighboring hexagon.

rochlore Heisenberg model.[83] In that case a lattice distortion was invoked to lift the degeneracy between the two singlet states of each tetrahedron.

2.5 Summary of the properties of VBC phases

The generic features of VBC (whatever the dimensionality of the lattice) are:

- A spin gap, no $SU(2)$ symmetry breaking and short-ranged spin-spin correlations,
- Long-ranged order in dimer-dimer and/or larger $S = 0$ plaquettes. The coupling of this order to lattice distortions is probable in experimental realizations of spontaneous VBC.
- In *spontaneous* VBC phases the ground-state is degenerate. From the theoretical point of view the discrete symmetry of the order parameter of the VBC which spontaneously breaks a lattice symmetry may give birth to a finite temperature Ising-like transition.[84] Simultaneity between this transition and a possible structural transition is likely when the couplings of the spins to the lattice degrees of freedom (phonons) is considered.
- VBC have gapped excitations, in the $S = 0$ sector as well as in other S sectors. A wide zoology of modes is to be expected as well as continua associated to multi-particle excitations or scattering of domain walls (in the case of a spontaneous symmetry breaking of the ground-state). In two dimensions all these excitations have integer spins (the ordered back-ground inducing a confinement of the spin- $\frac{1}{2}$ excitations)

Frustration on the square lattice or more generally on bipartite lattices is often overcome by VBC phases. No theorem forbids the appearance of VBC in triangular geometries but there is up to now no examples of such phases in pure spin- $\frac{1}{2}$ models (in next sections, examples will be given within the framework of quantum dimer models).

It has been advocated in the large- N approaches[43, 44, 45, 46] that, in two dimensions, classical collinear spin-spin correlations generically lead to VBC or VBS and only non-collinear spin-spin correlations can give birth to RVB SL with unconfined spin- $\frac{1}{2}$ excitations. The present knowledge of $SU(2)$ phase diagrams supports this prediction. The VBC found so far numerically in $SU(2)$ spin models appear to be in regions of parameter space where the spin-spin correlations are characterized by some short-ranged collinear order in the large- S limit. The J_1 - J_2 model on the honeycomb lattice has a classical incommensurate phase in the regime of high frustration and there are some evidences that in the quantum phase diagram

the collinear phase is separated from the columnar VBC phase by a RVB SL.[18] The multiple-spin exchange (MSE) model on the triangular lattice is also believed to be a RVB SL[85] and the corresponding classical ground-states generically have non-coplanar spin configurations. Capriotti *et al.*[58] argued that the spin- $\frac{1}{2}$ square lattice J_1 - J_2 model could be a RVB SL. If confirmed, this would be the first counter-example to the general rule explained above. The Heisenberg model on the pyrochlore lattice might be an other counter-example[77].

2.6 A simple model of VBC with a critical point: the hard core quantum dimer model of Rokhsar and Kivelson on the square lattice

Looking for a model with a resonating valence bond ground-state, Rokhsar and Kivelson introduced in 1988 a quantum hard core model on the square lattice [86]. Their motivation was the description of systems with strongly coupled real-space Cooper pairs. At half filling these next-neighbor Cooper pairs can be seen as next-neighbor valence-bonds. Pauli principle and Coulomb interaction imply that these valence-bonds are spin 0, hard core objects. Insofar as the spin gap is large enough, it can be speculated that the manifold of low energy states is spanned by the linearly independent set of nearest neighbor valence-bond coverings⁶.

2.6.1 Hilbert space and Hamiltonian of quantum dimer models

The Hilbert space of the "quantum dimer" models is build from the different non overlapping dimer coverings of the lattice. In that context dimers are not exactly nearest neighbor valence bonds, insofar as 2 configurations with dimers in different positions are orthogonal. But the dimer coverings are supposed to be in one-to-one correspondance with the orthogonalized configurations of nearest neighbor valence-bonds.

The dynamics of the low lying singlet excitations⁷ of this model are described by the Hamiltonian \mathcal{H}_{dimer} :

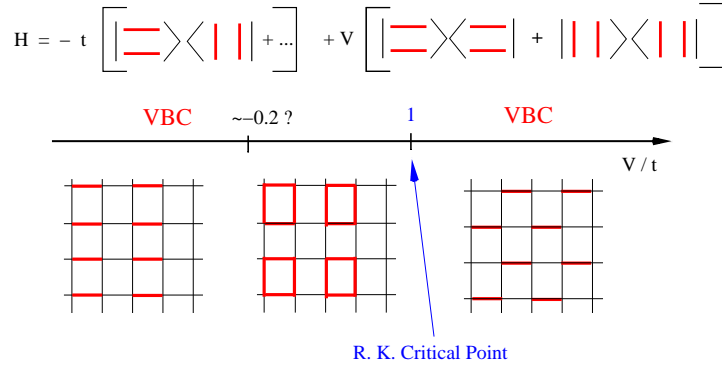
$$H_{dimer} = \sum_{\text{Plaquette}} [-J (|\uparrow\uparrow\rangle\langle\downarrow\downarrow| + h.c.) + V (|\uparrow\uparrow\rangle\langle\uparrow\uparrow| + |\downarrow\downarrow\rangle\langle\downarrow\downarrow|)] \quad (2.7)$$

See the original paper [86], or ref. [47] for the discussion of the derivation of this effective Hamiltonian from a more realistic Heisenberg or Hubbard model.

⁶It has been shown that such set form a family of non-orthogonal but linearly independent states [87, 59].

⁷By construction spin excitations are outside the scope of this modelization

Rokhsar–Kivelson hard core quantum dimer model
on the square lattice '88



Similar model on the hexagonal lattice: Moessner and Sondhi '01

Figure 2.8: Phase diagram of the Rokhsar Kivelson model on the square lattice

The first term of Eq. 2.7 describes the spatial flip of two parallel dimers from horizontal to vertical position and vice-versa, it could also be seen as a cyclic permutation of the two dimers around a square: it is a kinetic energy term which favors resonances between different configurations of parallel dimers (J is always > 0). The second term is a potential energy term likely to be repulsive in the original electron model. The ground-state for infinitely large $\frac{|V|}{J}$ is a Valence Bond Crystal, either staggered (for large $\frac{V}{J} > 0$), or columnar (for large $\frac{V}{J} < 0$). See Fig. 2.8.

2.6.2 Topological structure of the Hilbert space of the QDM model on the square lattice

The eigenstates of \mathcal{H}_{dimer} can be classified according to their winding numbers (Ω_x, Ω_y) across the 2-torus of the square sample with periodic boundary conditions. There are many equivalent ways to define these winding numbers. Let us follow RK. They draw the transition graph of a dimer configuration \mathcal{C} relative to a reference configuration \mathcal{C}_0 (which may be the columnar configuration) as the superposition of the dimer coverings of the two configurations \mathcal{C} and \mathcal{C}_0 . The dimers in \mathcal{C} are directed from one sublattice to the other and reversely for the dimers of \mathcal{C}_0 . The transition graph thus appears as a graph of oriented loops. The winding number Ω_x (resp. Ω_y) measures the net number of loops (clockwise minus counter-clockwise) encircling the torus in the x (resp. y direction). The Hamiltonian does not couple subspaces with different winding numbers. These pairs of wind-

ing numbers define N_s disconnected topological subspaces (where N_s is the number of lattice sites).

For $V \geq J \geq 0$, \mathcal{H}_{dimer} is positive semi-definite, the ground-state is unique at zero energy and nodeless (Frobenius theorem). Demons: A lower bond for the ground-state energy is given by a minimization of the Hamiltonian on each plaquette individually. If the given plaquette has no parallel dimer (non flippable plaquette), its energy is zero and if it has parallel dimers it has a potential energy V and at best a kinetic energy of $-J$. We can thus write a lower bond energy of the global system, which is proportional to the number of flippable plaquettes n_{flip} , as $\min [0, (V - J)n_{flip}]$.

2.6.3 Phase Diagram of the RK model

- The four staggered configurations are zero-energy eigenstates of \mathcal{H}_{dimer} . As they saturate the low energy bond, they are the ground-states for $V \geq J \geq 0$. They can be classified in two different topological classes in which they are the only representatives. They have a zero energy and any configuration of other topological subspaces has a larger strictly positive energy (at least of order $\mathcal{O}(L)$ in the limit $\frac{V}{J} \rightarrow \infty$).
- At the point $\frac{V}{J} = 1$ the model is exactly solvable. There is *in each topological subspace* a ground-state with zero energy. It is the equal amplitude superposition of all the configurations of that sector. *i)* Simple computation shows that these states are zero-energy states of \mathcal{H}_{dimer} . *ii)* Since all off-diagonal elements are non-positive the ground-state is unique and nodeless (Frobenius property, Marshall theorem). The equal amplitude states are thus the unique ground-states in their respective topological sectors. We will call these states the RK states.
- It has been shown by Kohmoto and Shapir [88], that the spin-spin correlations in this state decrease exponentially.
- An important property: any dimer correlation functions in the RK state can be computed from an exact mapping to the classical statistical problem of dimer coverings first solved by M. E. Fisher and J. Stephenson [89]. From this work one can conclude that the dimer-dimer correlation functions at $\frac{V}{J} = 1$, decreases algebraically with distance (as r^{-2}). This property implies that the first excitations above the ground-states are gapless.
- On the basis of the continuity in the energy between the staggered phase and the RK states, one may speculate that the RK point is the quantum critical end of the staggered VBC phase. But the excitations of the staggered VBC are non local and have energy of order $\mathcal{O}(N^{+0.5})$ in the $\frac{V}{J} \rightarrow \infty$ limit. To sustain the above point of view one should

explain how the kinetic term can dress these excitations so that they become gapless when $\frac{V}{J} \rightarrow 1$. In fact the more probable hypothesis is a first order phase transition between the RK phase and the staggered one. Such a question could perhaps be answered with Monte Carlo simulations.

- The ground-state wave-function at this RK point has a property which is considered as constitutive of a RVB spin liquid: that is resonances between all dimer coverings. It must be underlined here that this resonance phenomenon at the RK point does not bring any stabilization of the equal amplitude superposition ground-state when compared to the neighboring staggered VBC phase.
- RK then argue that for $\frac{V}{J} < 1$, there is, separated by a first order phase transition, a new phase which might be a “true” resonating Valence Bond Spin Liquid ⁸. The characterization of this phase is for the moment rather loose: RK argument is variational and rather weak. The first calculation by Sachdev on a 36 lattice [90], gives evidence for a VBC columnar state for $\frac{V}{J} < 0.5$ and not a clear conclusion nearer from the RK point. Extending the calculations to 64 sites, and using various estimators, Leung and co-workers [91] estimated that long range columnar order probably exists up to the RK point, with the restriction that up to $\frac{V}{J} \sim -0.2$ the order is very plausibly purely columnar, whereas in the range $-0.2 < \frac{V}{J} < 1$ the order could reduce to a 4-spin S=0 plaquette order. ⁹ The present consensus[92, 93] is for crystalline order everywhere except at the RK critical point.

In view of these results for the QDM model on the square lattice, of most studies on the $J_1 - J_2$ model, and of the $SU(N)$ studies on the same lattice [94, 43], one may be tempted to conclude that VBC is the paradigm of the quantum ground-state on square and possibly bipartite lattices. This might be untrue [58, 18], but the fact is that the triangular based lattices (see next chapters) seem much more favorable to Resonating Valence Bond Spin Liquids.

⁸i.e. a phase where the resonances between different dimer coverings are essential to its stabilization and are so important that there is a gap to the first excitations and any correlation functions: either spin-spin, dimer-dimer or higher order plaquette-plaquette correlation functions decrease exponentially with distance.

⁹This conclusion is not consistent with the degeneracy the authors claim for the ground-state. The nature of the phase for $\frac{V}{J} < 1$ remains an interesting but technically difficult open question.

Chapter 3

Resonating Valence Bond Spin Liquids

The Resonating Valence Bond Spin Liquid is a quantum concept introduced in 1973 by P. W. Anderson [95], following the line of thought of Linus Pauling for molecules. When the semi-classical Néel states or simple VBC are very far to satisfy each individual bond, Anderson speculated that the macroscopic system could take advantage of the *quantum resonances* between the *exponential number* of valence bond coverings to lower its ground-state energy. Such states have no long range order in any local order parameter whence the name of Spin Liquid: it is a Resonating Valence Bond Spin Liquid (abbreviated as RVB Spin Liquid or RVBSL in the following).

Spinons: As noted above the RVB phase has a gap to collective excitations, which is equally true of VBC. The major difference insofar between VBC and RVB Spin Liquids is the existence in this new quantum phase of deconfined spin-1/2 excitations: the spinons. If you break a Valence Bond in a VBC phase and try to separate the two single spins from each other the energy of the system increases as the length of the string of misaligned dimers which appears between the two single spins (take as an example the staggered or the columnar phase of the QDM). This creates an elastic restoring force which binds the two spin-1/2 together: in such a Valence Bond Crystals excitations have always an integer spin ($\Delta S = 0$ or 1). We thus infer that in the RVB Spin Liquid state, where the correlations between local operators are short range and any disordered configuration as probable as an other, the restoring force between two single spins beyond a certain distance will be negligible and the spin-1/2 (“spinons”) will be deconfined.

3.1 Introduction: short range versus long range Resonating Valence Bond wave-functions

Resonating Valence Bond wave-functions encompass a large class of wave-functions beyond the equal amplitude superposition of next neighbor valence bond coverings that we encounter at the RK point in the last chapter.

It is easy to verify that the whole set of valence bond coverings (without any restriction on the length of the valence bonds) is an overcomplete basis of the $S = 0$ subspace of the spin system (compare the numbers of these coverings to the size of the $S = 0$ subspace for a N site lattice).

Let us suppose that we have designed a family \mathcal{E} of linearly independent valence bond coverings \mathcal{C}_i , a general RVB wave-function will be written as:

$$|RVB\rangle = \sum_{\mathcal{C}_i \in \mathcal{E}} A(\mathcal{C}_i) |\mathcal{C}_i\rangle \quad (3.1)$$

where $|\mathcal{C}_i\rangle$ are products of valence bond wave-functions (with a sign conventionally fixed, respecting the lattice topology).

In variational calculations, one generally use restricted forms of Eq. 3.1, where the amplitude $A(\mathcal{C}_i)$ of a given configuration \mathcal{C}_i is written as the product of amplitudes $h(k, l)$ for each valence bond (k, l) present in \mathcal{C}_i .

Two situations have been studied:

i) either long range RVB wave functions where the function $h(k, l)$ depends algebraically on the distance r_{kl} between sites k and l (at least for large distances):

$$h(k, l) = \frac{Cst}{r_{kl}^\sigma} \quad (3.2)$$

Liang, Douçot et Anderson [5] have shown that such wave functions have Néel long range order in the Heisenberg model on the square lattice if $\sigma < 5$ and no Néel long range order for $\sigma > 5$ ¹. Capriotti and co-workers [58] have used a p -wave BCS wave-function for the $J_1 - J_2$ model on the square lattice, which has no long range order in valence bonds.

ii) or the short range Valence Bond w.-f. where the amplitudes $h(k, l)$ are not necessarily strictly restricted to next neighbors but decrease at least exponentially with distance (most of the following is concerned with that kind of wave functions). By construction such functions cannot describe Néel long range order, as Néel order has long range correlations between spins on the same sublattices. As we have seen in the previous chapter, this family encompasses the quantum critical behavior of the QDM model on the square lattice. Valence Bond Crystals can equally be described in this basis. BUT in the VBC case a few ordered configurations of dimers have a dominant weight in the thermodynamic limit. Many properties of

¹The ground-state of the rigid macro-antiferromagnet studied in the first chapter enters this class of wave functions with h uniform and of infinite range

these wave-functions have been studied theoretically ([96, 97, 98, 87, 59] and references therein), we will see some of them in the following.

In this chapter we will first describe with some length the properties of the QDM on the triangular lattice, to compare to the solution of the same model on the square lattice. We will then move to the exactly solvable QDM on the kagomé lattice introduced by Misguich, Pasquier and Serban[99, 100], which allows an intimate understanding of the vison wave-functions. A special attention will be given to the topological degeneracy of the ground-state, and to the existence of deconfined spin-1/2 “spinons” excitations, which is the most important experimental signature of a RVB Spin Liquid state.

3.2 The Quantum Dimer Model on the triangular lattice

The QDM model on the triangular lattice has been studied by Moessner and Sondhi in 2001 [93], when they realized that the dimer-dimer correlation function on this lattice was not algebraically decreasing as on the square lattice but *exponentially decreasing with distance*. The model on the triangular lattice comprises the same ingredients as on the square lattice: a potential energy term between parallel pairs of dimers and a kinetic energy term which does a cyclic permutation of parallel dimers on 4-spin plaquettes (involving two triangular units).

$$H_{dimer} = \sum_{\text{Plaquettes}} \left[-J \left(\left| \begin{array}{c} \text{---} \\ \text{---} \end{array} \right\rangle \left\langle \begin{array}{c} \text{---} \\ \text{---} \end{array} \right| + h.c. \right) + V \left(\left| \begin{array}{c} \text{---} \\ \text{---} \end{array} \right\rangle \left\langle \begin{array}{c} \text{---} \\ \text{---} \end{array} \right| + \left| \begin{array}{c} \text{---} \\ \text{---} \end{array} \right\rangle \left\langle \begin{array}{c} \text{---} \\ \text{---} \end{array} \right| \right) \right] \quad (3.3)$$

The sum over plaquettes runs on the three kinds of plaquettes with orientations at 60 degrees from each other.

J can be assumed to be positive²: it enforces resonance effects. V can be positive (repulsion between dimers) or attractive. The conditions of validity are the same as those of the model on the square lattice: it is supposed that the spin gap is large enough so that the first excitations are in the singlet sector. Insofar as the spin gap is large, the spin-spin correlations are short range which is consistent with the restriction to the subspace of nearest-neighbor Valence Bonds.

The properties of the lattice affect the properties of the QDM model on two central points:

- In the triangular case due to the higher entanglement of the lattice by the two-dimer permutation coupling, there are only 4 different topological sectors classified according to the parity of the winding numbers:

²This was not obvious a priori and is important in the following as it insures that the Hamiltonian is positive semi-definite for $V \geq J \geq 0$

(even, even), (even, odd), (odd, even), (odd, odd). (The dimer-flip term can change the winding numbers, not their parities).

- At temperature much larger than J and V , the classical square lattice problem has algebraically decreasing dimer-dimer correlations, whereas on the triangular lattice these correlations decrease exponentially [93].

As in the square lattice case, at the point $J = V$ the model is exactly solvable. The ground-states here too are the equal amplitude superpositions of all dimer coverings in each topological sector. (demonstration identical to the square lattice case). As in the square lattice case, these RVB states are degenerate with the 6 staggered configurations, which are ground-states for any $V/J \geq 1$ (see Fig. 3.1).

The sum over all configurations of the equal amplitude wave-functions is equivalent to the classical dimer problem (up to the question of the staggered phase which has a negligible statistical weight in the problem): thus the dimer-dimer correlations decrease exponentially with distance at the point $J = V$. Monte-Carlo simulations [93] have shown that this phase extends at least in the range $2/3 < V/J \leq 1$. It terminates at $V/J = 1$, with a first order transition to the staggered phase (seen in the Monte Carlo simulations as hysteretic behaviors). The dimer-dimer correlation function is very short range in all the above-mentioned range of parameter, and very weakly dependent on temperature, which is suggestive of a gap in the singlet spectrum. It's the description of a true RVB Spin Liquid phase with exponentially decreasing spin-spin and dimer-dimer correlations, and translational invariance of the ground-state (all four topological ground-states, with equal amplitude wave-functions are in the same $\mathbf{k} = (0, 0)$ sector of the impulsion [59]).

Topological degeneracy and quantum bits The 4-fold degeneracy of the g.-s. of a RVB on a 2-torus is a specific topological property of the true RVB Spin Liquid, associated to the genus of the surface on which the spins are living. On a cylinder such a g.-s. is doubly degenerate, *a priori* the most perfect illustration of quantum bit protected from any local perturbation and thus from most of the causes of decoherence. A. Kitaev was the first to discuss this subject [101]. Ioffe and collaborators [102] studied the effect of disorder on this topological bit. Misguich and coll. [103] discussed the time duration of a process of writing and reading such a q-bit and how finite size effects may be used to achieve this operation.

Two more complex evidences of RVB Spin Liquids phases had been obtained before the exhibition of this simple toy model: the first in 1992 in a large N $Sp(N)$ model by Sachdev [104], the second in a more realistic $SU(2)$ spin model by Misguich and coworkers [105, 85] ⁽³⁾

³See also cond-mat/0502464 : Lecture notes on Frustrated Quantum Magnets " Ecole

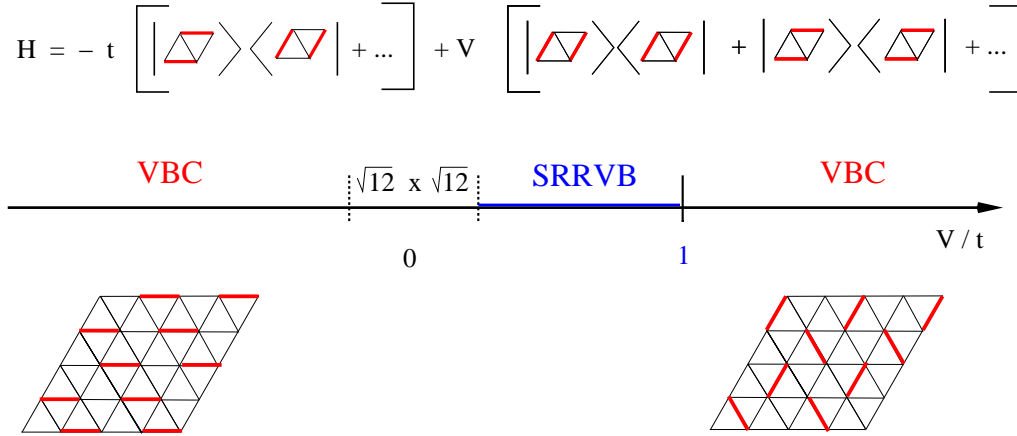


Figure 3.1: The phase diagram of the Quantum Hard Core Dimer problem on the triangular lattice after Moessner and Sondhi [93]

3.3 Solvable QDM on the kagome lattice

An exactly solvable QDM on the kagome lattice was introduced G. Misguich, D. Serban and V. Pasquier [99]. It offers a very simple and explicit realization of the ideas discussed above (visons, topological order etc.). In this section I strictly follow the presentation of Misguich [47], and include it here for completeness.

3.3.1 Hamiltonian

The kagome lattice QDM introduced in Ref. [99] contains only kinetic terms and has no external parameter. The Hamiltonian reads:

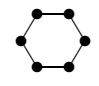
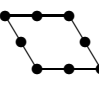
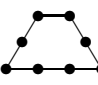
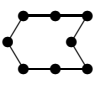

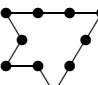
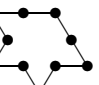

$$\mathcal{H} = - \sum_h \sigma^x(h) \quad (3.4)$$

$$\text{where } \sigma^x(h) = \sum_{\alpha=1}^{32} |d_\alpha(h)\rangle \langle \bar{d}_\alpha(h)| + \text{H.c} \quad (3.5)$$

The sum runs over the 32 loops on the lattice which enclose a single hexagon and around which dimers can be moved (see Table 3.1 for the 8 inequivalent loops). The shortest loop is the hexagon itself, it involves 3 dimers. 4, 5 and 6-dimers moves are also possible by including 2, 4 and 6 additional triangles (the loop length must be even). The largest loop is the star. For each loop α we associate the two ways dimers can be placed along that loop: $|d_\alpha(h)\rangle$ and $|\bar{d}_\alpha(h)\rangle$. Notice that $\sigma^x(h)$ measures the relative phases

de troisieme cycle de Suisse Romande" (2002)

Table 3.1: The 8 different classes of loops which can surround an hexagon of the kagome lattice. Including all possible symmetries we find 32 possible loops. The first column indicates the number of dimers involved in the coherent motion around the hexagon.

3			
4			
5			
6			

of dimer configurations displaying respectively the $d_\alpha(h)$ and $\bar{d}_\alpha(h)$ patterns in the wave function.

3.3.2 RK ground-state

As for the QDM discussed previously the ground-state of this Hamiltonian is the equal amplitude superposition of all dimer coverings belonging to a given topological sector (as on the triangular lattice there are four sectors). This can be readily shown by writing \mathcal{H} as a sum of projectors:

$$\mathcal{H} = -N_h + \sum_h \sum_{\alpha=1}^{32} [|d_\alpha(h)\rangle - |\bar{d}_\alpha(h)\rangle] [\langle d_\alpha(h)| - \langle \bar{d}_\alpha(h)|] \quad (3.6)$$

where N_h is the number of hexagons on the lattice. When expanding the products the diagonal terms give a simple constant since

$$\sum_{\alpha=1}^{32} |d_\alpha\rangle \langle d_\alpha| + |\bar{d}_\alpha\rangle \langle \bar{d}_\alpha| = 1 \quad (3.7)$$

This reflects the fact that, for any dimerization, the dimers on hexagon h match *one and only one* of the 2×32 patterns $\{d_\alpha, \bar{d}_\alpha\}$.

Unlike the square or triangular case, the RK ground-states $|0\rangle = \sum_{c \in \Omega} |c\rangle$

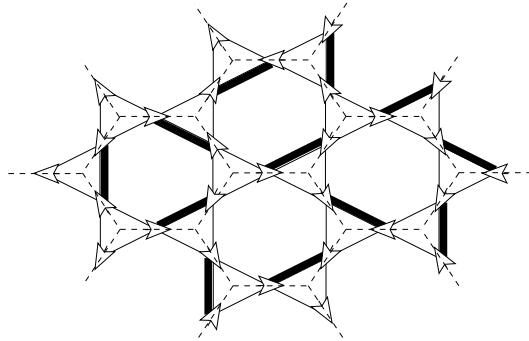


Figure 3.2: A dimer covering on the kagome lattice and the corresponding arrows. Dashed lines: honeycomb lattice.

are not degenerate with some staggered VBC.⁴ This means that the Hamiltonian of Eq. 3.4 is not at a phase transition to a VBC. As we will explain it is *inside* a liquid RVB phase.

The RK wave-function can be viewed as dimer condensate. It is similar to the ground-state of liquid ⁴He which has the same positive amplitude for any configuration and its permuted images.[106, 107] An important difference, however, is that the QDM state is incompressible and cannot sustain acoustic phonons. This can be related to the fact that the $U(1)$ symmetry of the Bose liquid is absent in the QDM on non-bipartite lattices. It is replaced instead by a discrete \mathbb{Z}_2 gauge symmetry (see §3.3.7 below).

3.3.3 Ising pseudo-spin variables

The kinetic energy operators σ^x defined in Eq. 3.5 commute with each other. This is obvious when two such operators act on remote hexagons but it also holds for neighboring ones. This property can easily be demonstrated with the help of the arrow representation of dimer coverings introduced by Zeng and Elser.[108] This mapping of kagome dimerizations to arrows on the bonds of the honeycomb lattice is illustrated Fig. 3.2. Each arrow has two possible directions: it points toward the interior of one of the two neighboring triangles. If site i belongs to a dimer (i, j) its arrow must point toward the triangle the site j belongs to. A dimer covering can be constructed from any arrow configuration provided that the number of outgoing arrows is odd (1 or 3) on every triangle.

The operators σ^x have a particularly simple meaning in terms of the arrow degrees of freedom: $\sigma^x(h)$ flips the 6 arrows sitting on h .⁵ It is then

⁴Because resonances loops of length up to 12 are present the dynamics is ergodic in each of the four topological sectors.[99]

⁵Flipping all the arrows around any closed loop (such as around an hexagon) pre-

clear that the σ^x commute and that $\sigma^x(h)^2 = 1$. In fact these operators can be used as Ising pseudo-spin variables and the Hamiltonian now describes non-interacting pseudo-spins in a uniform magnetic field pointing in the x direction. In the ground-state we have $\sigma^x(h) = 1$ on every hexagon.

3.3.4 Dimer-dimer correlations

The ground-state is the most possible disordered dimer liquid as the dimer-dimer correlations strictly vanish beyond a few lattice spacings. Such correlations can be computed by the Pfaffian method. On the kagome lattice the determinant of the Kasteleyn matrix (which is directly related to the partition function of the classical dimers problem) is exactly constant in Fourier space. Since dimer-dimer correlations are obtained from the Fourier transform of the inverse of this determinant, they turn out to be strictly zero beyond a few lattice spacings (as soon as the two bonds do not touch a common triangle).[99] This result can also be obtained by a simpler argument[99, 100] using the σ^x operators. This result is related to the kagome geometry.⁶ This absence of long-ranged dimer-dimer correlations demonstrates that the RK state is a dimer liquid and that it breaks no lattice symmetry.

On the triangular lattice, even at high temperature, dimer-dimer correlations decay exponentially with distance but these correlations remain *finite* at any distance. On the square lattice such correlations are even larger because they decay only as a power law. This means that the infinite hard-core dimer repulsion makes QDM non-trivial even at infinite temperature; dimers cannot be free when they are fully-packed. From this point of view we see that the kagome lattice is particular: it is as close as possible to a free dimer gas, except for non-trivial correlations over a few lattice spacings. This is a reason why dimer coverings on the kagome lattice can be handled with independent pseudo-spin variables and why the RK state on this lattice is the most possible disordered RVB liquid.

3.3.5 Visons excitations

The σ^x operators can be simultaneously diagonalized but they must satisfy the global constraint $\prod_h \sigma^x(h) = 1$ since this product flips every arrow *twice*. It must therefore leave all dimerizations unchanged. The lowest excitations have therefore an energy 4 above the ground-state and they are made of a *pair* of hexagons a and b in a $\sigma^x(a) = \sigma^x(b) = -1$ state. a and b are the locations of two Ising vortices (or *visons*[109, 110]). As remarked before this means that the relative phases of the configurations with $d_\alpha(h)$ and

serves the local constraint imposed on arrow configurations. Flipping the arrows around a topologically non-trivial loop changes the topological sector.

⁶The model of Eq. 3.4 can be generalized to any lattice made of corner-sharing triangles.[99]

$\bar{d}_\alpha(h)$ patterns have now changed sign. The corresponding wave-function is obtained in the following way. Consider a string Ω which goes from a to b (see Fig. 3.3) and let $\Omega(a, b)$ be the operator which measures the parity ± 1 of the number of dimers crossing that string. $\Omega(a, b)$ commutes with all $\sigma^x(h)$, except for the ends of the string: $\sigma^x(a)\Omega(a, b) = -\Omega(a, b)\sigma^x(a)$. A dimer move changes the sign of $\Omega(a, b)$ if and only if the associated loop crosses the string an odd number of times, which can only be done by surrounding one end of the string. This shows that $\Omega(a, b)$ flips the σ^x in a and b .⁷ As the RK ground state $|0\rangle$, $\Omega(a, b)|0\rangle$ is a linear combination of all dimer configurations belonging to one sector. However the amplitudes are now 1 and -1 depending on the number of dimers crossing Ω . This wave-function therefore has nodes, it is an excited state of energy 4 with two vortices in a and b . It is easy to see that a different choice Ω' for the string connecting a and b gives the same state up to a global sign which depends on the parity of the number of kagome sites enclosed by $\Omega \cup \Omega'$.

These vortex excitations carry a \mathbb{Z}_2 charge since attempting to put two vortices on the same hexagon does not change the state. Such excitations are not local in terms of the dimer degrees of freedom. Indeed, determining the sign of a given dimerization in a state with two visons which are far apart requires the knowledge of the dimer locations along the whole string connecting the two vortex cores. In this model the visons appear to be static and non-interacting. This is a particularity of this solvable model but the existence of gapped vison excitations is believed to be a robust property of RVB liquids. In more realistic models the visons will acquire a dynamics and a dispersion relation but will remain gapped.⁸ They will also have some interactions with each other but should remain *deconfined*. This property is particularly clear in the kagome QDM: visons are necessarily created by pairs but the energy is independent of their relative distances.

The Ising vortices also offer a simple picture of the topological degeneracy. Consider a ground-state $|+\rangle$ of the model which lives in the sector where the winding number Ω_y (with respect to some arbitrary but fixed dimerization) is even. Another ground-state $|-\rangle$ is obtained in the odd- Ω_y sector. Now consider the combination $|0\rangle = |+\rangle + |-\rangle$ and apply the operator $\Omega(0, L_x)$ corresponding to a closed loop surrounding the torus in the x direction. This amounts to creating a pair of nearby visons at the origin, taking one of them around the torus in the x direction and annihilating them. This can also be viewed as the creation of a vison in one hole of the torus (with no energy cost). It is simple to check that $\Omega(0, L_x)|0\rangle = |+\rangle - |-\rangle$ (up to an irrelevant global sign). This provides a simple relation between the vison-pair creation operator and the existence of two topologically distinct

⁷Up to a global sign (reference dependent) $\Omega(a, b)$ is equal to $\sigma^z(a)\sigma^z(b)$ where the σ^z operators are those introduced by Zeng and Elser.

⁸It is possible to add potential energy terms to Eq. 3.4 to drive the system outside of the liquid phase and this transition corresponds to a vison condensation.

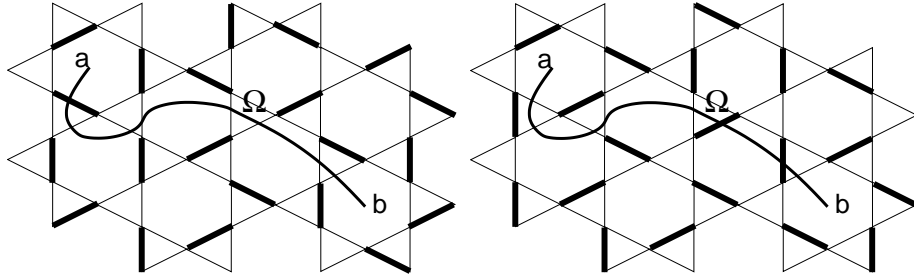


Figure 3.3: A pair of visons (located in a and b) is created by applying to the RK wave-function a factor (-1) for each dimer crossing the string Ω . The dimerization shown there on the left appears in the linear superposition of the two-vison state with the sign -1 whereas the one on the right has the sign $+1$.

ground-states $|+\rangle + |-\rangle$ and $|+\rangle - |-\rangle$.

3.3.6 Spinons deconfinement

We always assume that dimers represent “dressed” singlet valence-bonds. Since the Hilbert space is made of fully-packed dimer coverings the model of Eq. 3.4 only describes spin-singlet states. However, as any QDM, it can be extended to include static holes or spinons. Configurations with unpaired sites (spinon or holon) are now allowed but the kinetic terms of the original Hamiltonian which loop passes on an empty site gives zero. Consider a system with two static spinons in x and y . As on the square[86] and triangular lattices[93] at the RK point the exact ground-state $|x, y\rangle$ remains the sum of all dimer coverings and the ground-state energy is independent of the distance between the two spinons (except at very short distance if they belong to a common hexagon). This is a first indication that RVB *spin* liquid has deconfined spin- $\frac{1}{2}$ excitations (spinons). In the QDM language these excitations are simply unpaired sites in a dimer liquid background. Such unpaired sites are necessarily created by pairs but they can then propagate freely (no attractive potential) when they are sufficiently far apart.

Another calculation allows to test the deconfinement properties of a dimer liquid. We consider the state $|\psi\rangle = \sum_{\mathbf{r} \neq 0} |0, \mathbf{r}\rangle$ where $|0, \mathbf{r}\rangle$ is the (un-normalized) state with two spinons in 0 and \mathbf{r} . The probability to find a spinon in \mathbf{r} in the $|\psi\rangle$ can be obtained by the relatively involved calculation of the monomer correlation⁹ with Pfaffians. On the square lattice this probability goes to zero as $1/\sqrt{r}$. [89] This shows that the second spinon is (quasi-) confined in the vicinity of the first one on the square lattice because

⁹Ratio of number of dimer coverings with two holes in 0 and \mathbf{r} to the number without hole.

escaping far away represents a large “entropy” cost in the dimer background. On the triangular lattice it goes exponentially to a constant.[111] This result is a signature of deconfinement. In fact the same signature can be obtained on the kagome lattice without any technical calculation since the monomer correlation is exactly $1/4$ at any distance.footnoteThis follows from the independence of the arrow variables, see §V.B of Ref.[100].

If unpaired sites are allowed one can describe spinons or holons. Unfortunately in the presence of simple kinetic energy terms for these objects the model can no longer be solved. However one can consider a static spinon and its interaction with visons: when the spinon is adiabatically taken around a vison the dimers are shifted along a path encircling the vison. Because the vison wave-function is particularly simple in this model it is easy to check that this multiplies the wave-function by a factor -1 . This is the signature of a long-ranged statistical interaction[98, 112] between visons and spinons (or holons). In more realistic models, as long as the visons are gapped excitations the spinons are expected to be deconfined. On the other hand if the visons condense their long-ranged statistical interaction with spinons frustrates their motion. This is no longer true if they propagate in *pairs*, in which case they are not sensitive any more to visons (see Ref. [99] for an extension of the present QDM with a vison condensation). This simple physical picture illustrates the relation between vison condensation and spinon confinement.

3.3.7 \mathbb{Z}_2 gauge theory

The forces responsible for confinement are usually associated to gauge fields and their fluctuations. Whereas $U(1)$ compact gauge theories are generically confining in $2 + 1$ dimensions,[113, 114] \mathbb{Z}_2 gauge theories are known to possess deconfined phases.[115] For this reason some attention has been paid to the connexions between \mathbb{Z}_2 theories and fractionalized phases in 2D electronic systems.[109]

It is known[116] that QDM can be obtained as special limits of \mathbb{Z}_2 gauge theories, the gauge variable being the dimer number on a bond. However, on the kagome lattice this connexion can be made exact and completely explicit since there is a one to one correspondence between dimer coverings and physical states (*i.e.* gauge-invariant) of a \mathbb{Z}_2 gauge theory.[99] In this mapping the gauge fields are Ising variables living on the link of the honeycomb lattice (*i.e.* kagome sites) and are constructed from the arrows described previously. As for the constraints of gauge invariance they correspond to the odd parity of the number of outgoing arrows on every triangles. The σ^x operator used to define a solvable QDM translate into a gauge-invariant plaquette operator for the gauge degrees of freedom (product of the Ising gauge variables around an hexagon). With this mapping the visons appear to be vortices in the \mathbb{Z}_2 gauge field and the solvable model of Eq. 3.4 maps

to the deconfined phase of the gauge theory.

3.4 Summary of properties of RVB Spin liquids

- A RVB Spin liquid is a phase which does not break either $SU(2)$ symmetry nor any spatial symmetries of the lattice. Its ground-state is **unique** up to a topological degeneracy which exists only in systems with an odd number of spin-1/2 in the unit cell, living on a 2-torus (more generally the degeneracy is 2^g , with g the genus of the torus). In that sense it is awkward to call such a phase a disordered phase! None of the classical ideas associated to disorder are relevant to understand the properties of this RVB Spin Liquid phase. If we have to compare it to a liquid phase it is more the superfluid phase of 4He that we should have in mind!
- All correlation functions in local observables have only short range order, and consequently the susceptibility associated to any local observable is zero at $T=0$. In its ground-state this phase is an ideal q-bit (See A. Kitaev Lectures).
- This phase has a gap for all excitations, either in the singlet or the triplet sectors and it supports fractionalized excitations (the “spinons”). The first excitations in the singlet sector correspond in the gauge theory language to the bosons of the gauge field that Senthil and M. P. A. Fisher call “visons” [117, 118]. Due to the properties of the excitations we expect them to form continua in the spin sectors. The neutron experiment of Coldea and co-workers on Cs_2CuCl_4 is perhaps the first experimental proof of such a state [119].
- An RVB spin liquid state is expected in presence of competing and frustrating interactions. The bandwidth in which this phenomenon can be observed is in general strongly reduced and often only a small fraction of the original couplings: the case of the MSE system at $J_1 = -2$ and $J_4 = 1$ (the point where all the results given here have been calculated) is in some sense rather exceptional, as at this point the spin gap is almost as large as the cyclic 4-spin exchange.

Bibliography

- [1] B. Bernu, P. Lecheminant, C. Lhuillier, and L. Pierre, Phys. Rev. B **50**, 10048 (1994).
- [2] E. H. Lieb and D. Mattis, J. of Math. Phys. **3**, 749 (1962).
- [3] Hulthen, Ark. Mat. Astron. Fys. **26A**, 1 (1938).
- [4] W. Marshall, Proc. Roy. soc. London **A 232**, 48 (1955).
- [5] S. Liang, B. Doucot, and P. Anderson, Phys. Rev. Lett. **61**, 365 (1988).
- [6] P. Anderson, Phys. Rev. **86**, 694 (1952).
- [7] B. Bernu, C. Lhuillier, and L. Pierre, Phys. Rev. Lett. **69**, 2590 (1992).
- [8] P. Lecheminant, Ph.D. thesis, Université Pierre et Marie Curie, Paris, 95.
- [9] M. Gross, E. Sanchez-Velasco, and E. Siggia, Phys. Rev. B **39**, 2484 (1989).
- [10] M. Gross, E. Sanchez-Velasco, and E. Siggia, Phys. Rev. B **40**, 11328 (1989).
- [11] H. Neuberger and T. Ziman, Phys. Rev. B **39**, 2608 (1989).
- [12] D. Fisher, Phys. Rev. B **39**, 11783 (1989).
- [13] P. Azaria, B. Delamotte, and D. Mouhanna, Phys. Rev. Lett. **70**, 2483 (1993).
- [14] P. Hasenfratz and F. Niedermayer, Z. Phys. B. Condensed Matter **92**, 91 (1993).
- [15] D. C. Mattis, *The Theory of Magnetism I*, Vol. 17 of *Springer Series in Solid-State Sciences* (Springer-Verlag, Berlin, Heidelberg, New York, Tokyo, 1981).
- [16] W. J. Caspers, *Spin Systems* (World Scientific, Singapore, 1989).

- [17] A. Auerbach, *Interacting electrons and Quantum Magnetism* (Springer-Verlag, Berlin Heidelberg New York, 1994).
- [18] J.-B. Fouet, P. Sindzingre, and C. Lhuillier, *Eur. Phys. J. B* **20**, 241 (2001).
- [19] P. Tomczak and J. Richter, *Phys. Rev. B* **59**, 107 (1999).
- [20] N. Trivedi and D. Ceperley, *Phys. Rev. B* **41**, 4552 (1990).
- [21] C. Waldtmann *et al.*, *Eur. Phys. J. B* **2**, 501 (1998).
- [22] J.-B. Fouet, M. Mambrini, P. Sindzingre, and C. Lhuillier, *Phys. Rev. B* **67**, 054411 (2003).
- [23] J. C. Domenge, rapport de DEA, Magistere des Sciences de la matière de Lyon, 2002 (unpublished).
- [24] A. Sütö and P. Fazekas, *Phil. Mag.* **35**, 623 (1977).
- [25] G. Levine and J. Howard, *Phys. Rev. Lett.* **75**, 4142 (1995).
- [26] O. Waldmann, L. Zhao, and L. K. Thompson, *Phys. Rev. Lett.* **88**, 066401 (2002).
- [27] T. Guidi *et al.*, *Phys. Rev. B* **69**, 104432 (2004).
- [28] O. Waldmann *et al.*, *Phys. Rev. Lett.* **92**, 096403 (2004).
- [29] J. Villain, R. Bidaux, J. Carton, and R. Conte, *J. Phys. Fr.* **41**, 1263 (1980).
- [30] E. Shender, *Sov. Phys. J.E.T.P.* **56**, 178 (1982).
- [31] T. Oguchi, H. Nishimori, and Y. Taguchi, *J. Phys. Soc. Jpn.* **54**, 4494 (1985).
- [32] C. L. Henley, *Phys. Rev. Lett.* **62**, 2056 (1989).
- [33] E. Dagotto and A. Moreo, *Phys. Rev. Lett.* **63**, 2148 (1989).
- [34] T. Jolicoeur, E. Dagotto, E. Gagliano, and S. Bacci, *Phys. Rev. B* **42**, 4800 (1990).
- [35] A. Chubukov and T. Jolicoeur, *Phys. Rev. B* **46**, 11137 (1992).
- [36] S. E. Korshunov, *Phys. Rev. B* **47**, 6165 (1993).
- [37] R. Deutscher and H. Everts, *Z. Phys. B. Condensed Matter* **93**, 77 (1993).

- [38] P. Lecheminant, B. Bernu, C. Lhuillier, and L. Pierre, Phys. Rev. B **52**, 6647 (1995).
- [39] A. Luchli *et al.*, Phys. Rev. Lett. **95**, 137206 (2005).
- [40] N. Shannon, T. Momoi, and P. Sindzingre, Phys. Rev. Lett. **96**, 027213 (2006).
- [41] A. F. Andreev and I. A. Grishchuk, Sov. Phys. JETP **60**, 267 (1984).
- [42] P. Chandra and P. Coleman, Phys. Rev. Lett. **66**, 100 (1991).
- [43] N. Read and S. Sachdev, Phys. Rev. Lett. **62**, 1694 (1989).
- [44] N. Read and S. Sachdev, Phys. Rev. B **42**, 4568 (1990).
- [45] N. Read and S. Sachdev, Phys. Rev. Lett. **66**, 1773 (1991).
- [46] S. Sachdev, Reviews of Modern Physics **75**, 913 (2003).
- [47] G. Misguich and C. Lhuillier, in *Two-dimensional quantum antiferromagnets*, edited by H. T. Diep (World-Scientific, Singapore, 2005), cond-mat/0310405.
- [48] T. Senthil *et al.*, Science **303**, 1490 (2004).
- [49] P. Anderson, *Basic Notions of Condensed Matter Physics* (Benjamin, New York, 1984).
- [50] C. K. Majumdar and D. K. Ghosh, J. of Math. Phys. **10**, 1392 (1969).
- [51] P. Lecheminant, in *One-dimensional Spin Liquids*, edited by H. T. Diep (World-Scientific, Singapore, 2005).
- [52] A. A. Nersesyan and A. M. Tsvelick, Phys. Rev. Lett. **78**, 3939 (1997).
- [53] H. Schulz and T. A. L. Ziman, Europhys. Lett. **8**, 355 (1992).
- [54] M. E. Zhitomirsky and K. Ueda, Phys. Rev. B **54**, 9007 (1996).
- [55] V. N. Kotov, J. Oitmaa, O. Sushkov, and Z. Weihong, cond-mat/9912228 (unpublished).
- [56] V. N. Kotov, J. Oitmaa, O. Sushkov, and Z. Weihong, Phys. Rev. B **60**, 14613 (1999).
- [57] L. Capriotti and S. Sorella, Phys. Rev. Lett. **84**, 3173 (2000).
- [58] L. Capriotti, F. Becca, A. Parola, and S. Sorella, Phys. Rev. Lett. **87**, 097201 (2001).

- [59] G. Misguich, C. Lhuillier, M. Mambrini, and P. Sindzingre, *Eur. Phys. J. B* **26**, 167 (2002), cond-mat/0112360.
- [60] K. Ueda, H. Kontani, M. Sigrist, and P. A. Lee, *Phys. Rev. Lett.* **76**, 1932 (1996).
- [61] M. Albrecht and F. Mila, *Phys. Rev. B* **53**, 2945 (1996).
- [62] M. Troyer, H. Kontani, and K. Ueda, *Phys. Rev. Lett.* **76**, 3822 (1996).
- [63] S. Sachdev and N. Read, *Phys. Rev. Lett.* **77**, 4800 (1996).
- [64] O. A. Starykh *et al.*, *Phys. Rev. Lett.* **77**, 2558 (1996).
- [65] Z. Weihong *et al.*, *Phys. Rev. B* **55**, 11377 (1997).
- [66] H. Kageyama *et al.*, *Phys. Rev. Lett.* **82**, 3168 (1999).
- [67] H. Nojiri *et al.*, *J. Phys. Soc. Jpn.* **68**, 2906 (1999).
- [68] S. Miyahara and K. Ueda, *Phys. Rev. Lett.* **82**, 3701 (1999).
- [69] H. Kageyama *et al.*, *Phys. Rev. Lett.* **84**, 5876 (2000).
- [70] A. Koga and N. Kawakami, *Phys. Rev. Lett.* **84**, 4461 (2000).
- [71] E. Müller-Hartmann, R. R. P. Singh, C. Knetter, and G. S. Uhrig, *Phys. Rev. Lett.* **84**, 1808 (2000).
- [72] K. Totsuka, S. Miyahara, and K. Ueda, *Phys. Rev. Lett.* **86**, 520 (2001).
- [73] A. Laeuchli, S. Wessel, and M. Sigrist, *Phys. Rev. B* **66**, 014401 (2002).
- [74] K. Kodama *et al.*, *Science* **298**, 395 (2002).
- [75] S. Miyahara and K. Ueda, *J. Phys. Cond. Matt.* **15**, R327 (2003).
- [76] S. Palmer and J. Chalker, *Phys. Rev. B* **64**, 094412 (2002).
- [77] E. Berg, E. Altman, and A. Auerbach, *Phys. Rev. Lett.* **90**, 147204 (2003).
- [78] I. Affleck, T. Kennedy, E. Lieb, and H. Tasaki, *Phys. Rev. Lett.* **59**, 799 (1987).
- [79] I. Affleck, T. Kennedy, E. H. Lieb, and H. Tasaki, *Commun. Math. Phys.* **115**, 477 (1988).
- [80] M. den Nijs and K. Rommelse, *Phys. Rev. B* **40**, 4709 (1989).
- [81] T. Kennedy and H. Tasaki, *Phys. Rev. B* **45**, 304 (1992).

- [82] K. Hida, J. of the Phys. Soc. of Japan **69**, 4003 (2000).
- [83] Y. Yamashita and K. Ueda, Phys. Rev. Lett. **85**, 4960 (2000).
- [84] P. Chandra, P. Coleman, and A. Larkin, Phys. Rev. Lett. **64**, 88 (1990).
- [85] G. Misguich, C. Lhuillier, B. Bernu, and C. Waldtmann, Phys. Rev. B **60**, 1064 (1999).
- [86] D. Rokhsar and S. Kivelson, Phys. Rev. Lett. **61**, 2376 (1988).
- [87] J. Chayes, L. Chayes, and S. Kivelson, Commun. Math. Physic. **123**, 53 (1989).
- [88] M. Kohmoto and Y. Shapir, Phys. Rev. B **37**, 9439 (1988).
- [89] M. E. Fisher and J. Stephenson, Phys. Rev. **132**, 1411 (1963).
- [90] S. Sachdev, Phys. Rev. B **40**, 5204 (1989).
- [91] P. Leung, K. Chiu, and K. Runge, Phys. Rev. B **54**, 12938 (1996).
- [92] E. Fradkin, in *Field Theories of Condensed Matter Systems, Frontiers in Physics*, edited by D. Pines (Addison-Wesley, USA, 1991).
- [93] R. Moessner and S. L. Sondhi, Phys. Rev. Lett. **86**, 1881 (2001).
- [94] I. Affleck and J. Marston, Phys. Rev. B **37**, 3774 (1988).
- [95] P. Anderson, Mater. Res. Bull. **8**, 153,160 (1973).
- [96] B. Sutherland, Phys. Rev. B **37**, 3786 (1988).
- [97] B. Sutherland, Phys. Rev. B **38**, 7192 (1988).
- [98] N. Read and B. Chakraborty, Phys. Rev. B **40**, 7133 (1989).
- [99] G. Misguich, D. Serban, and V. Pasquier, Phys. Rev. Lett. **89**, 137202 (2002).
- [100] G. Misguich, D. Serban, and V. Pasquier, Phys. Rev. B **67**, 214413 (2003).
- [101] A. Y. Kitaev, Annals Phys. **303**, 2 (2003), quant-phys/9707021.
- [102] L. B. Ioffe *et al.*, Nature **415**, 503 (2002), cond-mat/0111224.
- [103] G. Misguich, V. Pasquier, F. Mila, and C. Lhuillier, Phys. Rev. B **71**, 184424 (2005).
- [104] S. Sachdev, Phys. Rev. B **45**, 12377 (1992).

- [105] G. Misguich, B. Bernu, C. Lhuillier, and C. Waldtmann, Phys. Rev. Lett. **81**, 1098 (1998).
- [106] R. P. Feynman, Phys. Rev. **90**, 1116 (1952).
- [107] R. P. Feynman, Phys. Rev. **91**, 1291 (1953).
- [108] V. Elser and C. Zeng, Phys. Rev. B **48**, 13647 (1993).
- [109] T. Senthil and M. P. A. Fisher, Phys. Rev. B **62**, 7850 (2000).
- [110] T. Senthil and M. P. A. Fisher, Phys. Rev. Lett. **86**, 292 (2001).
- [111] P. Fendley, R. Moessner, and S. L. Sondhi, Phys. Rev. B **66**, 214513 (2002).
- [112] S. Kivelson, Phys. Rev. B **39**, 259 (1989).
- [113] A. M. Polyakov, *Gauge Fields and Strings* (Harwood Academic, New York, 1987).
- [114] E. Fradkin and S. H. Shenker, Phys. Rev. D **19**, 3682 (1979).
- [115] J. Kogut, Rev. Mod. Phys. **51**, 659 (1979).
- [116] R. Moessner, S. L. Sondhi, and E. Fradkin, Phys. Rev. B **65**, 024504 (2002).
- [117] C. Lannert, M. P. A. Fisher, and T. Senthil, Phys. Rev. B **63**, 134510 (2001).
- [118] T. Senthil and M. P. A. Fisher, Phys. Rev. B **63**, 134521 (2001).
- [119] R. Coldea, D. A. Tennant, A. M. Tsvelick, and Z. Tylczynski, Phys. Rev. Lett. **86**, 1335 (2001).